HIGHLIGHTS

- The engine oil needs to enhance its properties to reduce the wear on the piston.
- The addition of CNC-CuO nanoparticles in the engine improved thermophysical properties behaviour's performance at 0.5% concentration.
- The results can be beneficial for the heat transfer application, especially for tribological

Improving the Thermophysical Properties of Hybrid Nanocellulose-Copper (II) Oxide (CNC-CuO) as a Lubricant Additives: A Novel Nanolubricant for Tribology Application

Mohd Kamal Kamarulzaman[1], Sakinah Hisham[2], K. Kadirgama[2*], D. Ramasamy[3,] M.Samykano[3], R. Saidur[4, 5], and Talal Yusaf[6]

[1]Automotive Engineering Centre, Universiti Malaysia Pahang, Pekan 26600, Pahang, Malaysia.

[2] Faculty of Engineering Technology Mechanical and Automotive, Universiti Malaysia Pahang, Pekan 26600, Pahang, Malaysia.

[3]College of Engineering, Mechanical Department, Universiti Malaysia Pahang, Pekan 26600, Pahang, Malaysia.

[4] Research Center for Nano-Materials and Energy Technology (RCNMET), School of Engineering Technology, Sunway University, Bandar Sunway, Petaling Jaya 47500, Selangor, Malaysia.

[5] Department of Engineering, Lancaster University, Lancaster LA1 4YW, UK.

[6] School of Engineering and Technology, Central Queensland University; QLD Australia.

ABSTRACT

The primary objective of the present analysis is to investigate the thermophysical properties of hybrid nanocellulose and copper (II) oxide nanoparticles added to engine oil as a lubricant for piston ring-cylinder liner application. Kinematic viscosity, viscosity index (VI) and dynamic viscosity have been performed for measurement of properties at varying temperatures (ranging from 30°C to 90°C) and different concentrations (ranging from 0.1% to 0.9% volume concentration). Thermal characteristics have been measured using similar temperatures and concentrations to determine thermal conductivity and specific heat capacity. In the results, as the concentration of the CNC-CuO nanoparticle increases, the VI also increases. This proves the combination of CNC-CuO particles with engine oil improves the lubricity of the base oil concerning its viscosity by 44.3%-47.12%. The lowest and highest improvements in the dynamic viscosity were 1.34% and 74.81%. The highest increment of thermal conductivity ratio for the selected nanolubricant was 1.80566% in the solid concentration of 0.1% at 90 °C. The specific heat capacity of nanolubricant tends to reduce slightly with an increase in temperature. Overall, the addition of CNC-CuO nanoparticle in the engine improved thermophysical properties behaviour's performance at 0.5% concentration. The results can benefit the heat transfer application, especially tribological.

KEYWORDS

Thermophysical properties; Nanocellulose; Copper (II) oxide; Nanolubricant

ABBREVIATIONS

AlO_2	Aluminium oxide
TiO_2	Titanium oxide
CuO	Copper Oxide
MWCNT	Multi walled carbon nanotube
CNC	Cellulose Nanocrystal
EG	Ethylene glycol
SAE	Society of Automotive Engineer
SiO_2	Silica oxide
Cu	Copper
PAO	Polyalphaolefin
PTFE	Polytetrafluoroethylene
UV–vis	Ultraviolet
$ZnAl_2O_4$	Zinc aluminium oxide
ASTM	American Standard Testing Method
MoS_2	Molybdenum disulphate
MgO	Magnesium oxide
DSC	Differential scanning calorimeter
VI	Viscosity Index
C_p	Specific heat
CaO/Na2O	Calcium oxide/sodium oxide

1.0Introduction

The main benefits of nanolubricants are that they are resistant to temperature compared to conventional additives and restricted tribochemical reactions [1]. It is possible to use different kinds of nanoparticles, either organic or inorganic nanoparticles [2]. Organic nanoparticles mainly include polymers, exosomes, liposomes, protein-based nanoparticles, coal fly as, etc., while inorganic nanoparticles consist of silica nanoparticles, metal nanoparticles, carbon nanotubes, quantum dots and so forth [3-7]. Organic-inorganic, or hybrid, nanoparticles have caught the interest of researchers due to their potential applications because they can combine useful chemical, optical, and mechanical properties while retaining the various benefits of nanolubricants. The dispersion of these nanoparticles for tribological properties, such as Multi-Walled Carbon Nanotube (MWCNT) or the latest research organic nanoparticle using coal fly ash hybrid with different inorganic nanoparticles such as copper, alumina and silica, has piqued the interest of researchers and academics in recent years, as it leads to friction and wear reduction [10-12]. A hybrid nanoparticle comprises two or more nanoparticles that have been synthesized and distributed in a base lubricant [8]. The main goal of creating hybrid nanolubricants is to enhance the properties of materials so that they have significantly better rheological properties than individual conventional nanolubricants [9.

On the other hand, not so much literature reports on using Cellulose Nanocrystal (CNC) as a nanomaterial dispersant with any base fluid, particularly in lubricants. CNC is non-toxic, biodegradable, and has a large surface area and high strength [8]. Nanocellulose emerges as an inexpensive and sustainable polymer material with beneficial properties of oleophilic, optical transparency and mechanical performance, both as films and aerogels, with a directive toward biodegradable, renewable, sustainable and carbon-neutral polymer materials [9]. Nanocellulose-nanoparticle hybrid exploration is still relatively sporadic but has increased significantly since the multifunctional nanocellulose hybrid report [10, 11].

Nanotechnology has enhanced lubricant performance by using nanoparticles as additives in lubrication systems since the advent of nanotechnology. The qualities of the base oil can be enhanced or reduced by the additives present in the lubricating oil. The effect depends on the nanoparticles' features, such as shape, size, and volume fraction [12]. Many researchers reported improved viscosity changes in lubricating oil functionalised with nanoparticles. They investigated the impact of lubricant viscosity variation due to increasing nanoparticle additive concentrations and temperature [13-15]. They discovered substantial relationships between viscosity and temperature and nanoparticle concentration; increasing temperature reduced viscosity while increasing particle volume fraction increased viscosity of nano-lubricant. According to these investigations, increasing the temperature and nanoparticle size or lowering the nanofluid concentration reduces the nanofluid viscosity [16, 17]. Many publications in the literature assessed varied concentrations below 1% and beyond 2%, demonstrating that there is no optimal concentration for nanoparticles [18, 19].

Improved thermophysical properties of fluids, viscosity, thermal conductivity and specific heat capacity have recently emerged as one of the most challenging problems for researchers to solve. As a result, numerous research has been conducted on adding nanoparticles to increase the conductivity of various fluids [20, 21]. Researchers have also looked into the effects of various parameters on viscosity variations to study and analyze the thermophysical attributes of various fluids after combining nanoparticles, such as enhanced SAE40 oil with a mixture of MgO and MWCNT [22], enhanced 10W40 by CuO and MWCNT [23], Al_2O_3 and MWCNT for optimization goals [24, 25], CaO/Na_2O [26], clove-treated MWCNTs and Al_2O_3 [27].

Previously, studies on the thermophysical properties of engine oil performance using single component nanolubricants with CNC and CuO nanoparticles are available in the literature [18, 28-31]. However, as mentioned, a single nanofluid does not include all the characteristics compulsory for a specific purpose in some of the rheological and thermal properties [32]. Hence, recent development in nanofluids research has developed new nanolubricants with two or more types of nanoparticles dispersed in engine oil. The nanolubricant's purpose is to improve natural wear and friction. When nanoparticles are added to base oil, their concentration affects wear and friction. However, the concentration limitation must be considered because the lubricants already contain additives. More research is needed to improve the additive in lubricant, particularly on the concentration of additive used and the constraints involved. Various nanoparticle dispersions with differing nanoparticle material properties, shapes, sizes, and concentrations have been extensively studied in the last decade. Most of these studies have been carried out in polar base fluids like water, ethylene glycol (EG), and mixtures. [33-36]. This paper aims to evaluate the thermophysical properties of CNC-CuO nanolubricants for application in piston ring-cylinder liner contact for tribology application. This research is important, stating that only a few studies are available on organics-inorganics nanofluids based on manufacturing sector lubricants for viscosity and thermal applications. The considerably low stated results on lubrication-based nanofluids revolve around transformer oil, silicon oil, gear oil and heat transfer oil, and there are inadequate studies on engine lubricants-based nanofluids. Furthermore, the studies also revolve around single inorganic nanoparticles such as copper, aluminium, zinc oxide etc.

2.0 Methodology

2.1 Preparation of nanolubricant

SAE 40 was chosen as a base fluid for the nanolubricant. Blue Goose Biorefineries Inc was a provider for the CNC with a 7.4% water weight concentration, meaning the CNC is in gel form. Yuan, Fu [37] recommended spray drying as a suitable practice in drying the suspension of nanocellulose. Copper oxide nanoparticles look like brownish-black powder. It can be changed to metallic copper when reacting to hydrogen or carbon monoxide at high temperatures. The present study considered the parameter for concentration in volume per cent. Hence the conversion from weight concentration to volume concentration is required for CNC and CuO single components of nanolubricant. This study selected the two-step method to prepare nanolubricants, similar to the previous study. The Yu and Xie two-step approach prepares five different nanolubricant samples from 0.1% to 0.9% weight concentration. This technique consists of two steps: (i) nanoparticle production in powder form and (ii) nanoparticle dispersion in base fluids to generate a stable and homogeneous solution.

The CNC was synthesized into powder form to synthesise nanoparticles since its form is barely an off-white cream structure. To dry CNC from the suspension, water content from CNC suspension must be removed to sustain the nanofibrils size to the nanoscale. Since CNC is hydrophilic, the CNC melts at high temperatures and dissolves in any aqueous solvent [38]. A lab-scale blower was used for the spray drying process. It was also carried out at 25˚C relative temperature in an air-conditioning controlled room. The flakes form of CNC are rapidly produced as its suspension is evaporated from the hot air stream by the blower nozzle. The flakes are manually ground for about 60 minutes to get the even powder form via porcelain mortar.

For the dispersion of the nanoparticles into the base fluid, the nanolubricants were prepared at 70:30 CNC-CuO. The nanolubricants were prepared for different volume concentrations from 0.1 to 0.9% at an optimum composition ratio in stage one. The process flow and steps in the preparation of CNC-CuO nanolubricants as shown in Figure 1. Initially, in Step 1, the preparation of nanolubricants started with calculating the required volume for dilution using Equation 1.

$$\emptyset = \frac{\left[\frac{W_p}{\rho_p}\right]}{\left[\frac{W_p}{\rho_p} + \frac{W_{bf}}{\rho_{bf}}\right]} \qquad \text{Eq.1}$$

CNC and CNC-CuO nanolubricant were prepared with 0.1, 0.3, 0.5, 0.7 and 0.9% volume fraction in 200 ml of base oil SAE 40. Wp indicates the nanoparticles' weight (grams), (p indicates the density of the nanoparticles (g/cm3), (bf indicates the density for the base fluid in g/cm3, and Wbf indicate the base fluid weight (grams). CNC with CuO powder were then dry mixed to produce CNC-CuO nanoparticles. After that, the mixing process of nanoparticles in the base fluid was done by using a stirrer in Step 2. The nanolubricant was mixed up for 30 minutes, as suggested by other researchers [35, 39-42].

Hotplate magnetic stirrer was used for the initial dispersion process of CNC and CNC-CuO nanoparticles into engine oil at medium stirring rate continuously for 1 hour at room temperature. Each of the nanolubricant solutions then was left approximately for 2 hours in an ultrasonic bath. This was a very important step to intensify the stability of the nanolubricant. Furthermore, the sample of nanolubricants was subjected to the sonication process.

2.2 Stability Test for Nanolubricant

Floating nanoparticles tend to be clustered due to large surface area and surface reactions. It’s a fact that the stability and dispersibility of nanolubricants are two important criteria that affect their usage [39]. Various methods are used, such as sedimentation, centrifugation, zeta potential, and spectral absorbency. These methods are proposed to assess the stability of suspensions. For this paper, the sedimentation method and visual absorbency analysis are done to analyze the stability. A stable suspended nanoparticle is observed in the particle size of the supernatant particle as it remains constant in the solution. Several researchers have adapted the sedimentation method in their stability investigation [38, 40-43]. An 8 ml sample of nanolubricant was placed in the test tube at a stationary state. The camera captured the sample and compared it with the first day images over time. Then, the images of sedimentation over time for the nanolubricant were captured on the first day of preparation and up until 30 days. Images of the sedimentation behaviour changes and separation levels are recorded during this period.

UV-Visualisation spectrophotometer is a straightforward, quick and cost-effective method to quantitatively measure and characterize colloidal dispersion stability conditions. This method is based on fluids absorption and is useful for analysing different types of fluids dispersion but inappropriate for high volume concentrations of nanoparticle dispersion. In this experiment, the device functioned at a steady wavelength of 1200nm for every measurement of the nanolubricant sample. In this experiment, the Pelkin Elmer UV-Vis spectrophotometer (model number TGA 4000) with a wavelength range of 190 to 3300 nm was utilized in this investigation. The equipment has functioned at a steady wavelength of 1200 nm for an individual sample of nano lubricant. A transparent crystal cuvette is used to place the sample test inside the spaces. The spectrophotometer provides six sample slots for measurement with one slot for reference fluid, SAE 40, and another five for SAE 40. Before each measurement for precaution, the cuvette was carefully cleaned using distilled water to avoid contamination with the previous sample. UV-Vis spectrophotometer is utilized to determine the lessening light beam after reflection from a sample surface or passing through a sample. The scattering and absorption of light are determined by comparing the light power of the CNC-CuO nanolubricant. The absorbance of the light, when directed to the sample test, will show the existence of nanoparticles in the base fluid. In other words, densely populated nanoparticles in the base fluid are projected to show considerable absorbance and lower absorbance value due to fewer nanoparticles in the solution [44].

2.3 Kinematic and Dynamic Viscosity

Kinematic viscosity data was performed following the American Standard Testing Method (ASTM D445) through a temperature-constant bath of Cannon Instrument Company, United States of America (Model CT-500 Series II) utilizing Cannon-Fenske Routine Model crystal tube viscometer with 2 mm inner diameter together with, Cole-Parmer Polystat economical constant temperature bath at a temperature of 40℃. Thermal oil was utilized to obtain stable temperature distribution inside the tube at 40˚C, and 100˚C for individual concentrations were determined accordingly. The viscosity index (*VI*) calculates the difference in viscosity versus the temperature. *VI* is an arbitrary measure for viscosity variation with temperature differences. The VI values were determined according to the standard described in the American Society for Testing (ASTM D-2270), based on the determination of the kinematic viscosity. The VI is calculated from equation 2 below:

$$VI = 100\frac{L-U}{L-H} \qquad \text{Eq. 2}$$

where U is kinematic viscosity at 40˚C while L and H are the values found in the ASTM D2270 table from kinematic viscosity at 100˚C.

The viscosity of the lubricant is a significant indicator for lubricating testing. A commercial Brookfield DV-I prime viscometer was utilized to determine at dissimilar rotation speed (rpm). This viscometer can also be utilized in Newtonian and non-Newtonian liquids, ranging from small to large viscosity values (differing on the spindle, range of 1 to 600 cP); however, this instrument is precise for low viscosity fluids (ranged between 1 and 5 cP). The viscometer is a rotating type that uses a spindle submerged in the nanolubricant sample. The 25mL volume of nanolubricant was added to the chamber test and attached to the rheometer. Then the chamber and water jacket were carefully attached to the rheometer spring with the spring deflection within 2 to 3%. The nanolubricant sample was heated using a mixing water bath until reaching the required temperature. The dynamic viscosity values were observed for the temperature range of 30 to 90℃. A Rheocalc software was utilized for the current viscosity values. The viscosity was calculated by changing the speed of the spindle rotation. The measurement was done three times to get the average values. Then, the setup was validated by comparing the SAE 40 base oil at 30 to 90℃.

2.4 Thermal Conductivity and Specific Heat Capacity

KD2 Pro thermal property analyzer was used to measure the thermal conductivity of the CNC-CuO nanolubricant. A single needle sensor named KS-1 was selected for the thermal conductivity measurement. This sensor can measure the thermal conductivity of liquids in the range of 0.002 to 2.00 W/m.K. The needle for the KS-1 sensor was inserted into the sample bottle vertically at the centre and sealed with tape. Then the sample bottle of nanolubricant was immersed in the water bath for approximately 10 minutes until the temperature of the nanolubricants reached the bath temperature.

The KD2-Pro was calibrated using the Glycerin liquid provided by the manufacturer before the experiments were conducted. The average Glycerin thermal conductivity was recorded with 0.286W/mK at 25℃. The thermal conductivity was conducted for a temperature between 30°C to 90°C. The measurement was done three times, and the median value from three sets of data was obtained. The current thermal conductivity measurement is measured in 15 minutes by the following reading for each data set at various temperatures and volume concentrations. This step reduces the errors during thermal conductivity measurement due to the temperature change along the sensor in direct contact with the nanolubricant sample. The present thermal conductivity measurement followed the ASTM D5332-08 and IEEE 442-03 standards.

To determine the specific heat capacity of the nanolubricant, a differential scanning calorimeter (DSC), model DSC1000-/C from Linseis Messgeräte GmbH, Selb, Germany, was employed. This DSC follows the standard method ASTM E1269-11(2018). DSC is a thermal analysis technique examining how a material's heat capacity (Cp) is changed over temperature. This equipment gives the highest possible accuracy Cp by using heating rate temperature profiles. Nanolubricant is heated or cooled, and the changes in its heat capacity are tracked during changes in the heat flow. A furnace that can be heated up and cooled down homogenously is required to perform DSC. Two crucibles contain nanolubricant samples, and the other one is the empty crucible that acts as reference calorimeters that are equipped with high sensitive temperatures. When the furnace is heated at a constant rate, heat flows through the crucible of the nanolubricant sample and reference. The oven is purged with protective gas, nitrogen (N2), at a 24 ml/min flow rate. The usage of N_2 also avoids ice formation at low temperatures and the oxidation process. [45].

3.0Results and discussion

3.1 Stability of CNC-CuO nanolubricant

The sedimentation observation was done by capturing images within a certain period for the nanoparticles to sediment at the bottom of the test tube without any disruption. The length of this test differs from days to months. Peng et al. reported the deposit after 30 days for the silica and alumina nanoparticles scattered in paraffin lubricant [46]. In a different study by Sui et al. (2016), the permanence of the nanosilica enriched polyalphaolefin (PAO) lubricants was analyzed by storing the lubricants for 60 days [47]. Amiruddin et al. (2015) assessed the diffusion stability of SAE15W40 enhanced with nanohBN for 60 days. Dubey ran this test for 7 days in PTFE-based nanolubricants [48]. Thus, various test intervals have been stated by investigators for various nanoparticle and lubricant permutations. Hence, it is worth saying that the main idea for the selection of test time is based upon examining uncommon dispersion behaviours of lubricant samples. It can also be said that the test can be completed when the naked eye observes the deposits. The height of the solid-liquid interface of the supernatant layer of the samples was observed periodically. From the statement above, the period of observation was recorded at week one and at week 4. All samples were kept in test tubes and set aside undisturbed throughout the observation period and were observed periodically for any visual changes. Figure 1 shows the sedimentation observation in week 1. The samples were mixed well with no settlement of nanoparticles at the bottom of the test tube at week 1. After the 4th week, the supernatant layer is at the top of the solution. Therefore, CNC-CuO nano lubricant was observed to be stable for up to one month or more, as shown in Figure 2.

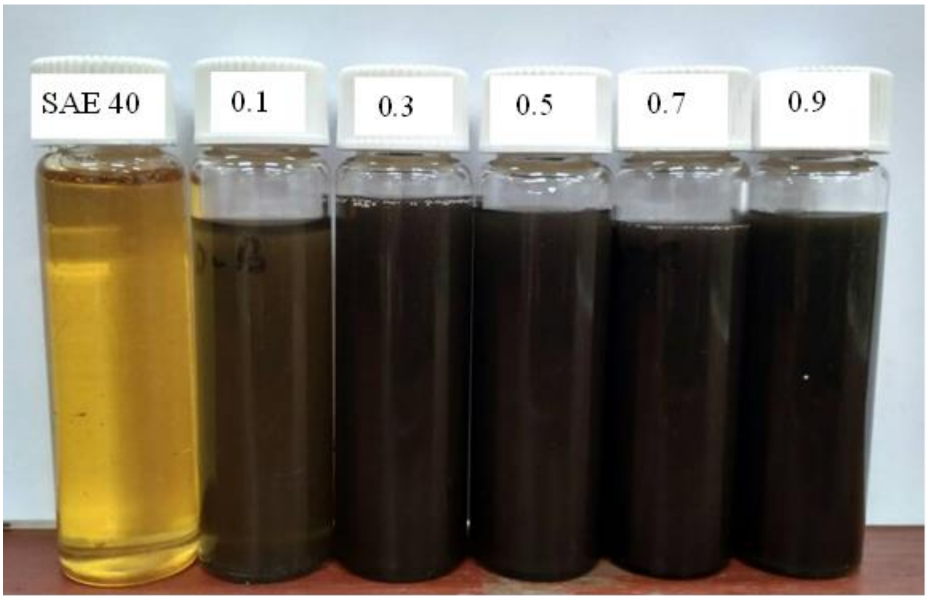

Figure 1 Sedimentation observation at week 1

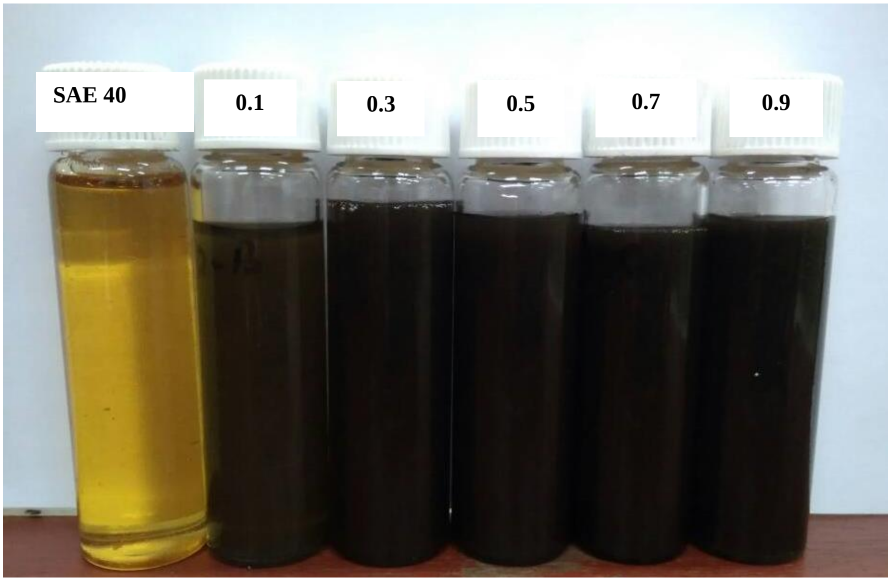

Figure 2 Sedimentation observation at week 4

Next presents the data UV-Vis spectrophotometer for CNC-CuO nanolubricants. The gamut pattern at numerous volume concentrations of CNC-CuO lubricant is shown in Figure 3. The peak absorbance can be seen from 0.1% to 0.5%. The peak position is broadened due to the increase in CNC-CuO nanoparticle concentration. As can see in Figure 3 as well, 0.7% and 0.9% show asymmetrical distribution due to the limitation of UV-Vis spectrometry. UV Vis functions well on liquid and solutions, but if the sample is made of a suspension of solid particles in liquid and has darker solutions, the sample scatters the light more; thus, the data obtained will be biased. Thus, it proves that 0.5% is the optimum concentration for CNC-CuO stability, and further experiments will only discuss three concentrations.

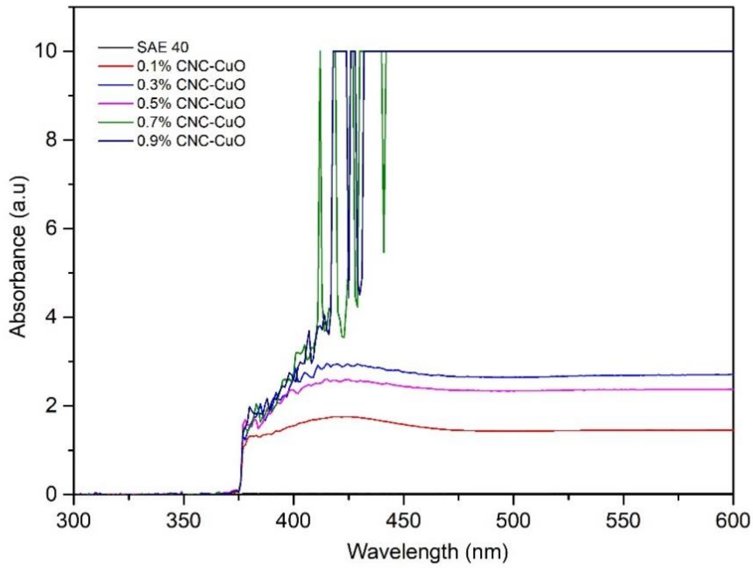

Figure 3 UV Vis spectrophotometer for CNC-CuO

As nanoparticles deposited in nanofluid, the absorbance in the supernatant part declined with concentration. The association among these two variables is stated as the Beer-Lambert law. The law states a linear relationship between the concentration and the absorbance of the liquid, which allows the concentration of a mixture to be determined by evaluating its absorbance [49]. This principle suggests that weightage intensity is linearly related to absorbance. As seen in Figure 4, the highest absorbance values of CNC-CuO nanolubricant with three distinct concentrations were found over a wavelength of 380-383 nm. Using corresponding absorbance values from each concentration, a linear correlation between absorbance and concentration of colloids was obtained, as shown in Figure 4, with the R^2 at 0.96494. This is as per the Beer-Lambert law.

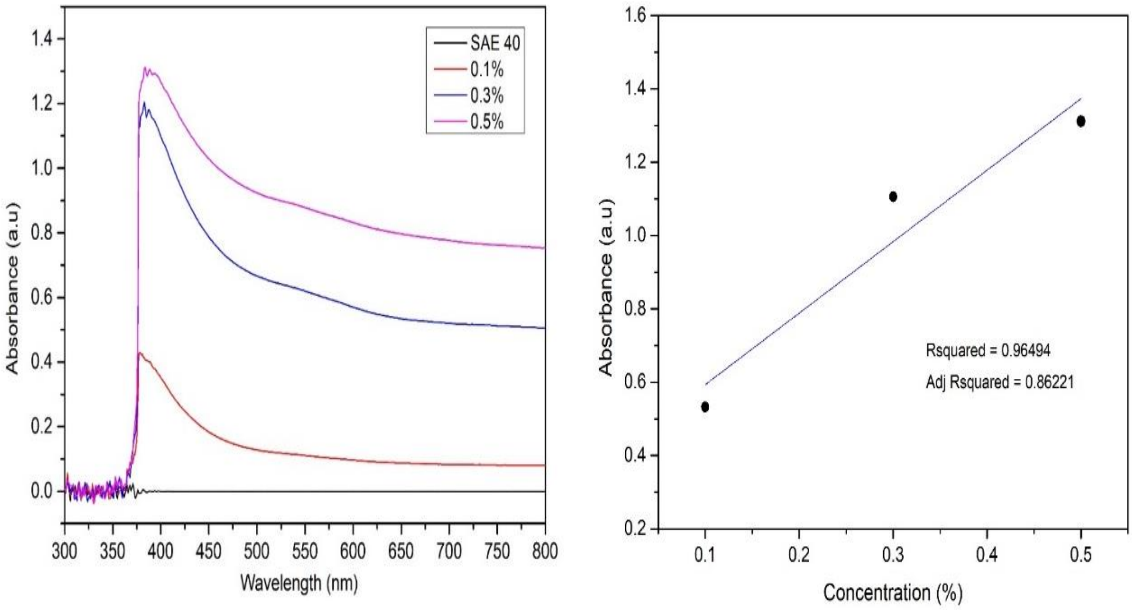

Figure 4 UV Vis spectrum for 0.1% to 0.9% concentration

Figure 5 shows the amount of the highest absorbance per week. It indicates that the small concentration of nano lubricants sediment is faster due to rapid agglomeration [50]. The absorbance ratio signals the ratio of the last absorbance at a specific sedimentation time to the initial absorbance of the mixture. The ideal absorbance ratio is 100%, representing good stability during the deposit period. As Hajjar et al. [51] discussed, the more the ratio is to 1 with the increase of the sedimentation times affect the stability of the test. Equation 3 determines the final absorbance ratio:

$$A_r = \frac{A}{A_o} \qquad \text{Eq.3}$$

where A_r denote the absorbance ratio, A denotes the final absorbance, while A_o denotes initial absorbance. According to Figure 6, 0.1% shows the closest absorbance ratio to one; thus, 0.1% concentration shows the most stable nanolubricant, followed by 0.5%, and the least stable nano lubricant is 0.3% concentration.

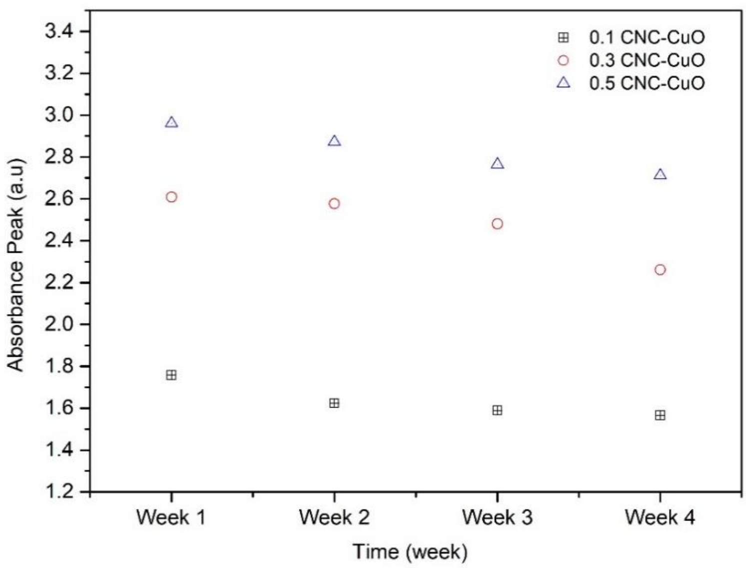

Figure 5 Absorbance peak for one month

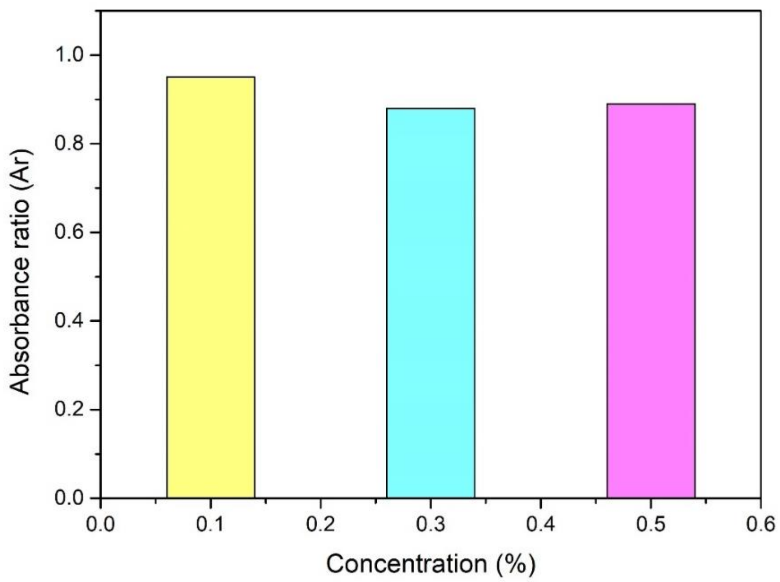

Figure 6 Absorbance ratio for 0.1%, 0.3% and 0.5% concentration.

3.2 Kinematic Viscosity and Viscosity Index

The main physical criteria for determining the condition of the oil is engine oil viscosity. The viscosity in a lubricant depends primarily on the operating temperature. Determining kinematic viscosity is vital for the ability of a lubricant to lubricate contact surfaces efficiently. Nanoparticle dispersion can greatly affect the viscosity of the base lubricant, which is a key factor in determining load-bearing potential and viscous friction [51] (Kotia, Borkakoti, & Ghosh, 2017). The viscosity of the base oil and various additive samples are taken out using Capillary Viscometer based on the ASTM D445 standard. In kinematic analysis, the concentration of nanoparticles in volume and temperature were evaluated as the two controllable parameters that were effective for engine oil. Kinematic viscosities were resolved at 40◦C and 100◦C.

Figure 7 shows the viscosity increment in percentage when CNC-CuO nanoparticles are added to the engine oil in different concentrations at 40℃ and 100℃. The mathematical relation for the viscosity increment measurement is calculated by using equation 4.

$$Viscosity\ Increment\ (\%) = \frac{Nanolubricant\ viscosity - Engine\ oil\ viscosity}{Engine\ oil\ viscosity} \times 100 \qquad \text{Eq.4}$$

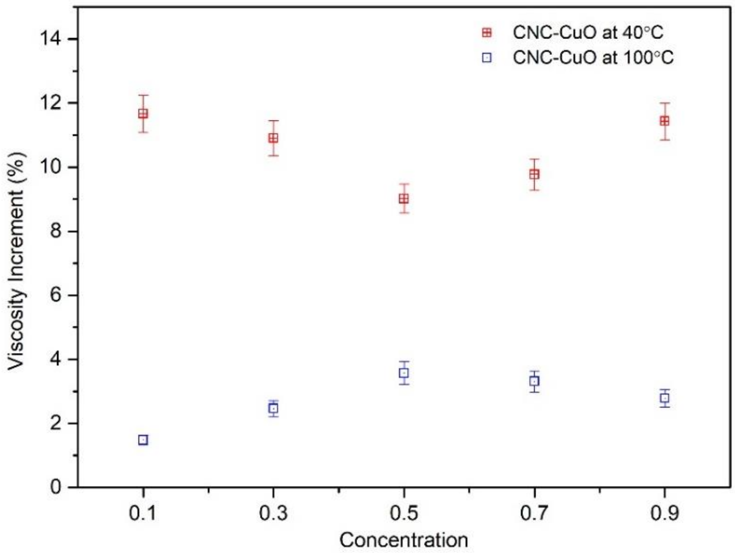

Figure 7 Viscosity increment at 40°C and 100°C

At 40°C, the viscosity increment decreases until 0.5% concentration and starts to rise at 0.7% concentration. In contrast with 100°C, the viscosity increment is increased to 0.5% and starts to decrease at 0.7% of CNC-CuO. The graph also shows that the viscosity of all lubricants reduces with the temperature rise. This is owing to the deterioration of the intermolecular strength of attraction among base fluid molecules [52]. The rise of nanoparticles in the liquid results in agglomeration on the surface, causing molecular collision. This improves nanolubricant viscosity. The collision of the molecular forces in increasing temperature reduces the viscosity of the nano lubricant [13]. The relative viscosity of nanolubricant with the change in temperature for various concentrations is shown in Figure 8. Equation 5 shows the mathematical relation for getting relative viscosity.

$$\mu_r = \frac{\mu_{nl}}{\mu_{bf}} \qquad \text{Eq.5}$$

μ_r is relative viscosity, μ_{nl} is nanolubricant viscosity, and μ_{bf} is base fluid kinematic viscosity. From the relation, it can be observed that the increment in relative viscosity depends on the fluid viscosity considered for the analysis.

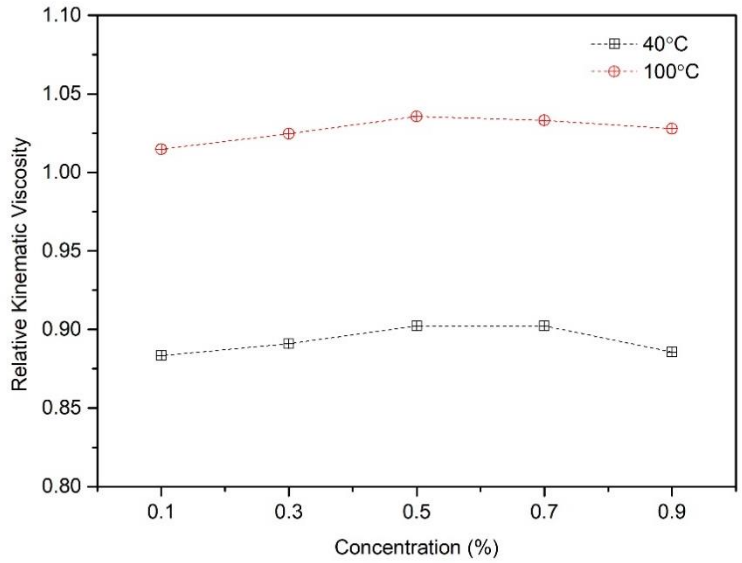

Figure 8 Relative kinematic viscosity at 40°C and 100°C

Figure 8 shows the maximum change for the 0.5% CNC-CuO nanoparticles concentration at the highest temperature of 100°C. When the fluid's viscosity increases with the addition of the nanoparticles, a higher value is observed in relative viscosity with 0.5% CuO nanoparticles addition [53]. Due to this viscosity reduction in relative kinematic viscosity at 0.5%, it was easy for nanoparticles to enter between the oil layers and the CNC and CuO nanoparticles acting as catalysts. Furthermore, the nanoparticles' almost spherical form influenced their rheological behaviour. Similarly, the viscosity of the CNC-CuO nanolubricant was only slightly reduced. Viscosity friction was reduced thanks to the low viscosity reduction. The low viscosity decrease helped to lessen viscous friction. The fewer viscosity decrease in the nanolubricants confirmed the CNC and CuO nanoparticle's effect on decreasing friction and thus lowering the frictional energy losses [54]. Oil viscosity is a required indication for lubricating analysis due the viscosity of a lubricant is directly linked to its ability to decrease friction on contact surfaces. Normally, a low viscous lubricant is desired [55]. The engine oil pump works with low energy to move a low viscous liquid. If the lubricant has a high viscosity, it requires a substantial amount of energy to work; oppositely, if it is too thin, the surfaces will come in contact, and friction increases [56]. The viscosity index (VI) was analysed to recognise which lubricant demonstrates better properties, as shown in Figure 9. The lower the VI, the better the viscosity difference of the oil with heat. Higher VI is required to demonstrate better friction and wear [57]. This proves that the CNC-CuO nanoparticle combined with engine oil improved the lubricity of the base oil viscosity by 44.3%-47.12%.

The higher viscosity index meant that it was more resistant to lubricant film thinning and had better fuel efficiency in an automotive engine. Figure 9 presents the viscosity of blended engine oil SAE 40 with CNC nanoparticles at increased concentration. It is clear that using nanoparticles of CNC and CuO as additives with blended engine oil also decreases the kinematic viscosity at 40°C and 100°C, which has considerably lower kinematic viscosities than engine oil SAE 40. It is also evident that the viscosity of nanolubricant decreases with increasing temperature. This is possibly due to a deterioration of attractive intermolecular forces that permits more rapid movement of suspended particles in the nano lubricants and offers less resistance to motion [58].

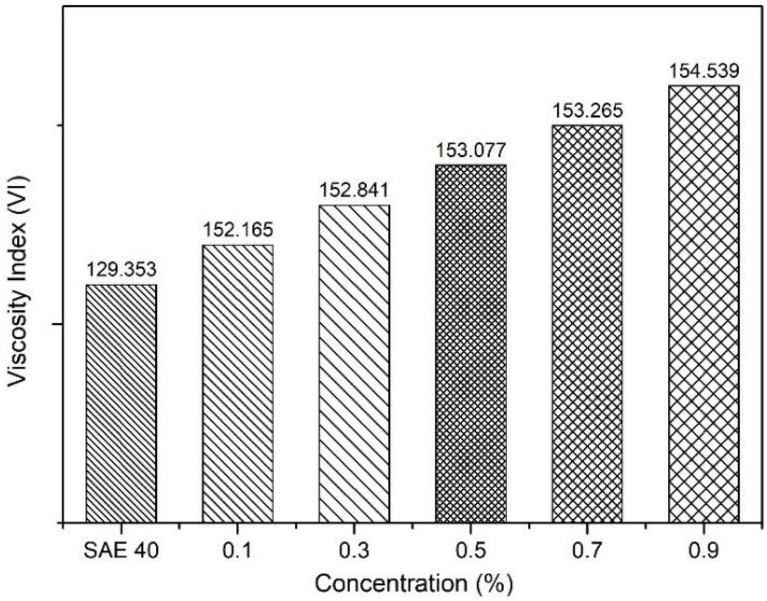

Figure 9 Viscosity index for CNC-CuO nanolubricant at all concentrations,

Figure 10 shows the comparison between CNC-CuO, CNC and Chaurasia et al. that use CuO nanoparticles as additives. The graph clearly shows that CNC-CuO shows the highest VI increment for all concentrations compared to other nanolubricant. The maximum VI increment was obtained at 0.9 concentration. The last changes in viscosity index increase were studied at lesser concentrations and temperatures. These variations happened due to a greater molecular collision rate at an elevated temperature [53]. There will be molecular interchange in a liquid similar to what occurs in a gas, but there are additional significant attractive, cohesive forces between the molecules of a liquid. Liquid viscosity is affected by both cohesion and molecular interchange. When the temperature of a liquid rises, it reduces the cohesive forces while increasing the rate of molecular interchange. The former causes a decrease in shear stress, whereas the latter causes an increase. As a result, as the temperature increases, the viscosity of liquids decreases. When temperatures rise, viscosity increases in gases and decreases in liquids and drag force decreases [59].

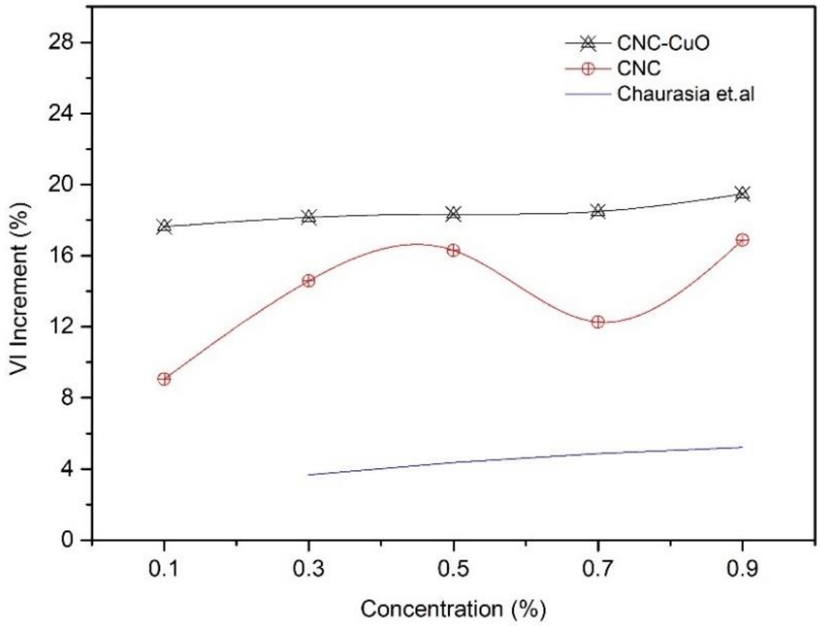

Figure 10 VI compares CNC-CuO and CNC nanolubricant with the previous researcher.

3.3 Dynamic Viscosity

The rheological behaviour of nanofluids is a concern to many researchers, whether it is Newtonian or Non-Newtonian fluids. For example, [60] reported that the viscosity directly depends on the shear rate, while in contrast, [61] suggested that the viscosity of nanofluid is impartial to the shear rate. Based on the statement, nanofluid's Newtonian or Non-Newtonian behaviour can be recognized by investigating the relation between shear stress and shear rate. According to Esfe et al., the recognition of Newtonian and Non – Newtonian fluid behaviour can be determined by its type of internal resistance, viscosity to shear rate [62]. The researcher in this approach investigated the dependence of viscosity on shear rate. Independence of fluid’s viscosity on the shear rate indicated that the fluid is similar to Newtonian fluids' behaviour. Still, viscosity dependency on shear rate suggests that fluid has a close behaviour to non- Newtonian fluids. Liquids in which viscosity reduces with rising shear rates are known as pseudoplastic fluids, while fluids in which viscosity rises with rising shear rate are called dilatant fluids.

Various discussions have been made on the rheological performance of nanofluids, whether it is Newtonian or non-Newtonian fluids. For example, [51] reported that the viscosity of a mixture containing Al2O3 is independent of the shear rate. At the same time, Kabelac and Kuhnke [60] indicated that the shear rate promptly impacts the viscosity of such a solution. Thus, recognizing whether the nanofluid is Newtonian or non-Newtonian is the first step to researching the rheological performance of CNC-CuO nanolubricant. The Newtonian behaviour of nanofluids can be expressed as follows:

$$\tau = \mu\gamma \qquad \text{Eq.6}$$

The shear stress of CNC-CuO nanolubricant concerning shear rate and temperature at the concentration of 0.1% has been shown in Figure 12. Where τ represents the shear stress, μ represents the dynamic viscosity, and γ represents the shear strain. Based on the figure, it can be assumed that under the circumstances of the present investigation, the studied nanolubricant exhibits Newtonian behaviour.

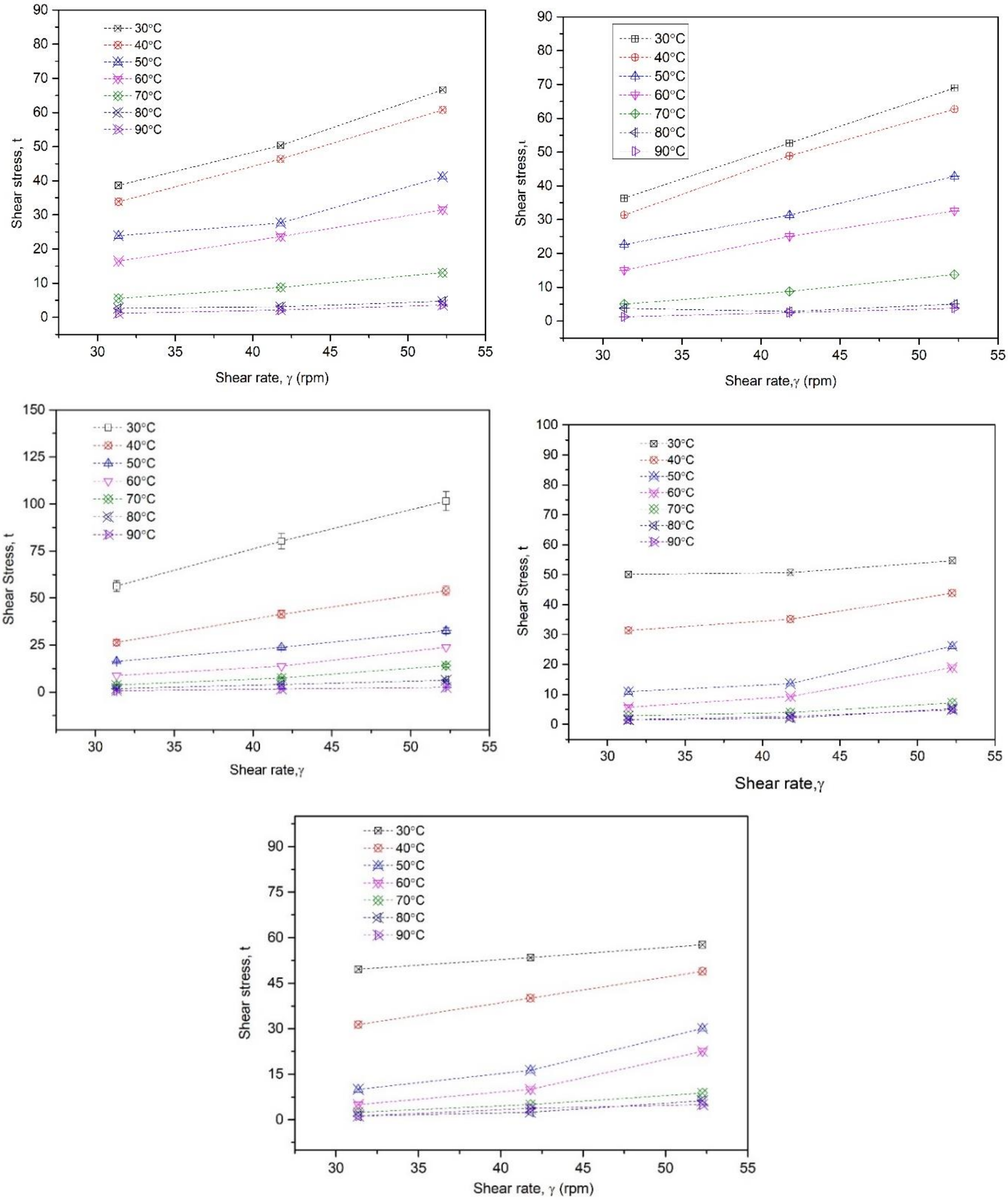

Figure 11 Variation of shear stress versus shear rate for CNC-CuO at a different concentration from 0.1% to 0.9%

3.3.1 Dynamic Viscosity in Different Temperatures and Concentration

Figure 12 displays the dynamic viscosity of CNC-CuO engine oil nanolubricant regarding temperature in different solid mixtures. Raising the temperature leads to lessening the dynamic viscosity of the examined nanolubricant in each solid concentration. It is to note that raising the solid concentration at a continuous temperature improves the nanofluid's dynamic viscosity. This rise is substantial in low temperatures contrasted to the higher ones. The dynamic viscosity of the examined nanolubricant concerning solid concentration in various temperatures has been displayed in Figure 13.

According to [63], viscosity is affected by the adhesive forces among liquid molecules. In accordance, the molecules are impacted by a larger quantity of energy at a greater temperature, affecting the adhesive forces. As a result, higher energy molecules can move more freely. The higher occurrence of molecular collision per unit volume and per unit time affects resistance against the movement of the liquid. Decreased intermolecular forces are driven by increased temperature and lower resistance to the liquid movement. Therefore, the viscosity of Newtonian nanofluid reduces with rising temperature. Brownian motion is another cause for switching the viscosity with the temperature and volume fraction. The impact of nanoparticles' Brownian movement on the nanofluid viscosity after the increasing temperature is understandable. Nanoparticles and the base fluid now have easy molecular movements, and the possibility of intermolecular collision is decreased in nanoparticles with the temperature rise. Moreover, the intermolecular gap between nanoparticles and the base fluid improves with the temperature rise, thus lowering the resistance to movement and viscosity.

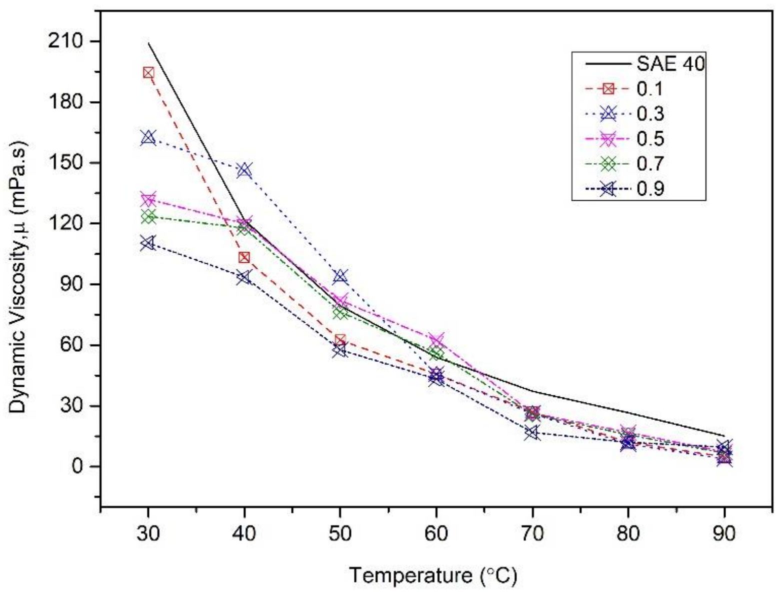

Figure 12 Dynamic viscosity at the increasing temperature at different concentration

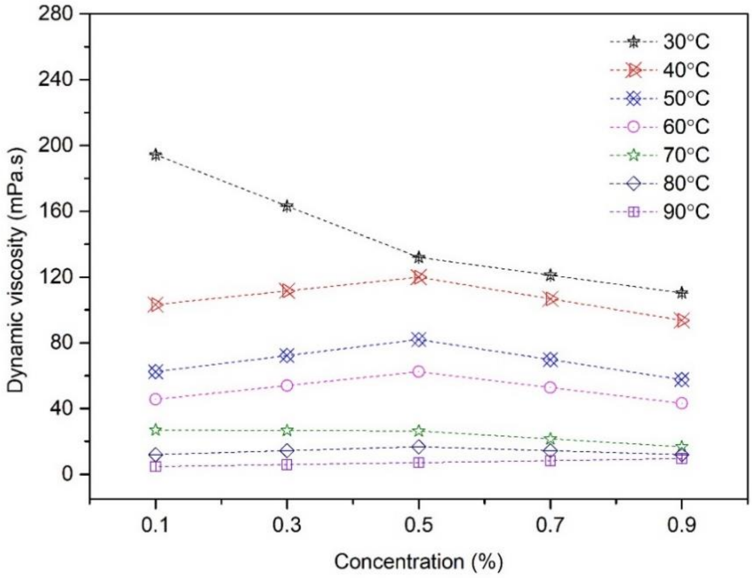

Figure 13 Dynamic viscosity at the increasing concentration for different temperature

Figure 14 shows the difference in viscosity improvement concerning temperature in several solid concentrations. The calculation of viscosity enhancement can be denoted as below:

$$Visosity\ enhancement, \% = \pm\left(\frac{\mu_{nl} - \mu_{bf}}{\mu_{bf}}\ x\ 100\right) \quad \text{Eq.7}$$

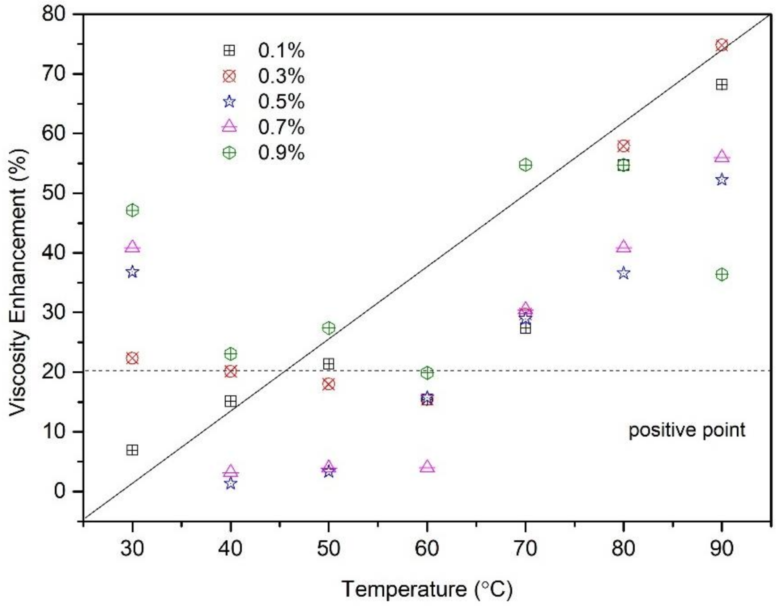

Figure 14 Viscosity enhancement at increasing temperature for different concentrations.

From Figure 14 that the maximum improvement in viscosity in solid concentrations of 0.3% at 90°C, while in solid concentrations of 0.25% and 0.5%, the highest rise occurred at the temperature of 35 °C. Hence, it's interesting to note that an increase in dynamic viscosity of the examined nanolubricant at a solid concentration of at all concentrations except 0.9% concentration at 40°C temperatures, 0.1% at 30°C, 0.7%, 0.5% and 0.9% at 60°C and 0.3%, 0.5% and 0.7% at 50°C was fewer than 20% which can be assumed as an optimistic fact in manufacturing and engineering application of this nanolubricant [64]. Thus, the minimum and maximum enhancement in the dynamic viscosity was 1.34% and 74.81%, which occurred at the temperature of 40°C and 90°C and solid concentrations of 0.5% and 0.3%, respectively

3.3.2 Difference Between Hypothetical Model and Experimental Data

Many hypothetical models to calculate the dynamic viscosity of nanolubricant have been suggested by researchers. In this analysis, 4 frequently used models are analysed; Einstein, Batchelor, Wang and Maiga are selected to examine their capability to calculate the dynamic viscosity of the examined nanolubricant and assess their results with the experimental data. Table 1 displays the selected theoretical models.

Table 1 Selected theoretical models to predict the dynamic viscosity

Model	Description	Proposed by
$\boldsymbol{\mu_{nf} = (1 + 2.5\varphi)\mu_{bf}}$	Foresee the viscosity of a suspension, including globular particles in solid concentrations less than 5%	[65]
$\boldsymbol{\mu_{nf} = (1 + 2.5\varphi + 6.2\varphi^2)\mu_{bf}}$	Foresee the dynamic viscosity of a suspension containing rigid globular particles	[66]
$\boldsymbol{\mu_{nf} = (1 + 7.3\varphi + 123\mu^2)\mu_{bf}}$	Foresee the dynamic viscosity of nanofluids	[67]
$\boldsymbol{\frac{\mu_{nf}}{\mu_f} = 1 - 0.19\varphi + 306\varphi^2}$	The relation was obtained by executing a least-square curve fitting method of experimental.	[68]

The contrast between the chosen theoretical models and experimental data is shown in Figure 15. Neither model can calculate the nanofluid's dynamic viscosity in an accurate value. Therefore, it is necessary to suggest a model that can calculate the nanofluid's dynamic viscosity in the appropriate accuracy range. Table 2 shows the error analysis between model from previous researcher compared to experimental data.

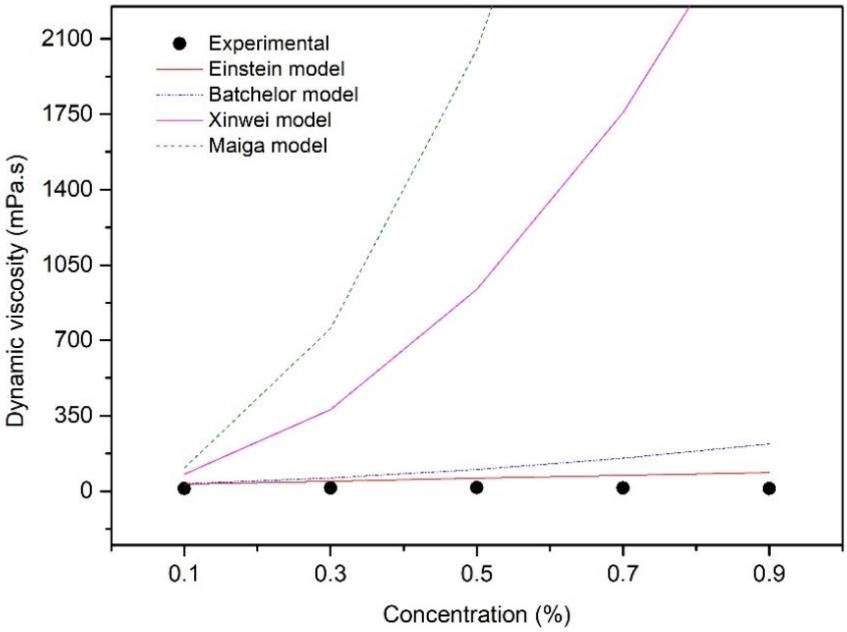

Figure 15 Comparison between theoretical models from previous researchers and current experimental data

Below are the error analysis compared to the previous model and experimental result.

$$\text{POAE (\%)} = \left(\frac{\text{Experimental value - Model value}}{\text{Experimental value}}\right) \times 100 \qquad \text{Eq.8}$$

Table 2: Error analysis between previous researcher model and experimental in percentage

Concentration	**Einstein Model**	**Batchelor Model**	**Xinwei Model**	**Maiga Model**
0.1	176.0625	189.7551667	553.716	792.4548333
0.3	222.0729167	324.7681944	2524.434167	5142.058819
0.5	254.9375	499.45	5484.35	12110.63875
0.7	406.1145833	965.2331944	12116.68583	27654.7716
0.9	617.7625	1726.871167	23575.12	54822.96567

3.4 Thermal Conductivity

The thermal conductivity of liquids is an important thermal property that influences heat transfer performance. The improvement in thermal properties of nanolubricants will drive the system to operate at utmost efficiency, especially in the internal combustion engine. Researchers attempted to enhance the reduced thermal conductivity of the standard heat transfer fluids by scattering several nanoparticles in the base fluid, mainly in engine oil [64, 69-71]. Therefore, the thermal conductivity enhancement of CNC-CuO nanolubricants was investigated under three conditions; (i) Different concentrations of nanoparticles dispersed in engine oil. (ii) Nanolubricants at optimum concentration with the variation of temperature, and (iii) Nanolubricants with various types of nanolubricant at constant volume concentration.

3.4.1 Thermal Conductivity in Different Temperatures and Solid Concentration

The thermal conductivity of CNC-CuO nanolubricant with different concentrations (0.1% to 0.9%) is defined with a temperature varying from 30℃ to 90℃. Figure 16 and Figure 17 show the temperature-related results of the thermal conductivity of the chosen nanoparticle proportions. According to both figures, the thermal conductivity value shows an erratic outcome as the temperature increases. With a concentration of 0.5%, the value of thermal conductivity at 50℃ has risen. The trend decreases gradually until 90℃. As for 0.9%, the thermal conductivity increases marginally up to 90℃. Hence, the combination between carbon-based nanoparticles (CNC) and metallic (CuO) as the thermal conductivity amount displays the consistent growth pattern for CNC nanolubricant, as shown in Figure 18.

In contrast, Aberoumand et al. show a consistent decreasing pattern for CuO nanolubricant [72, 73]. Despite the inconsistent pattern for CNC-CuO nanolubricant as the temperature increases, all concentrations for CNC-CuO nanolubricant show better results than the base fluid (SAE 40). This outcome is because the mean path between each of the nanoparticles was high when the nanolubricants were at smaller concentrations and higher temperatures, consequently reducing the collision probability. When the fluid heats, the Brownian movements of molecules strengthen and thus, the consequent interaction between the molecules increases. The fast motions of the particles due to an expansion in temperature also affect the clumping of the particles, which boosts the possibility of impacts among the particles. As a result, the improvement of the thermal conductivity. Another reason can be because the near-field radiation was strongly affected by the thermal conduction as the temperature of the nanolubricant increased [74].

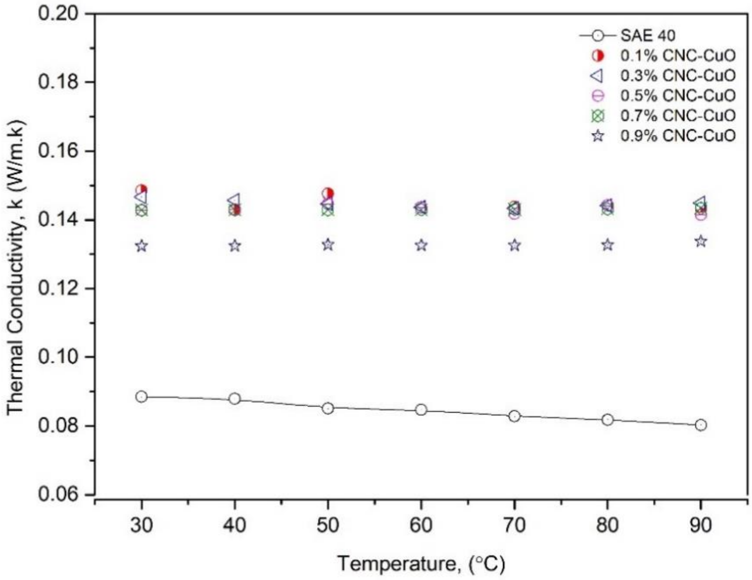

Figure 16 Thermal conductivity of CNC-CuO at different concentrations and increasing temperature

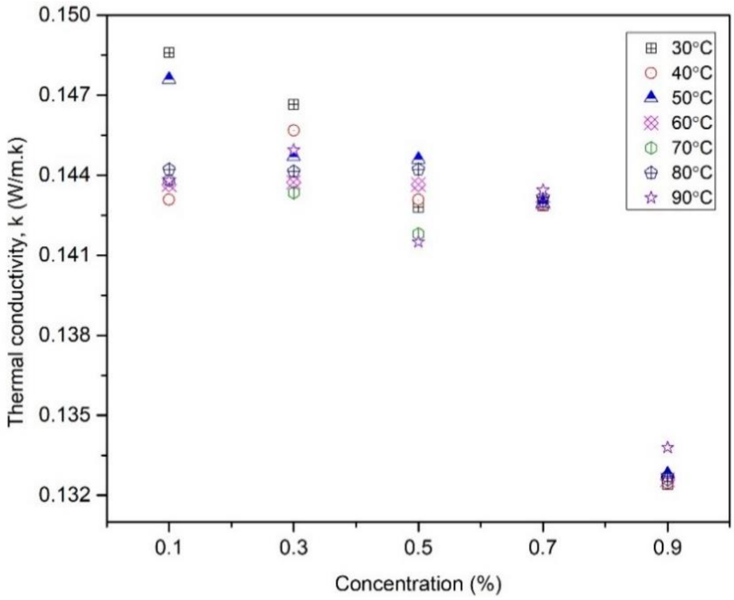

Figure 17 Thermal conductivity versus different concentrations at increasing temperature

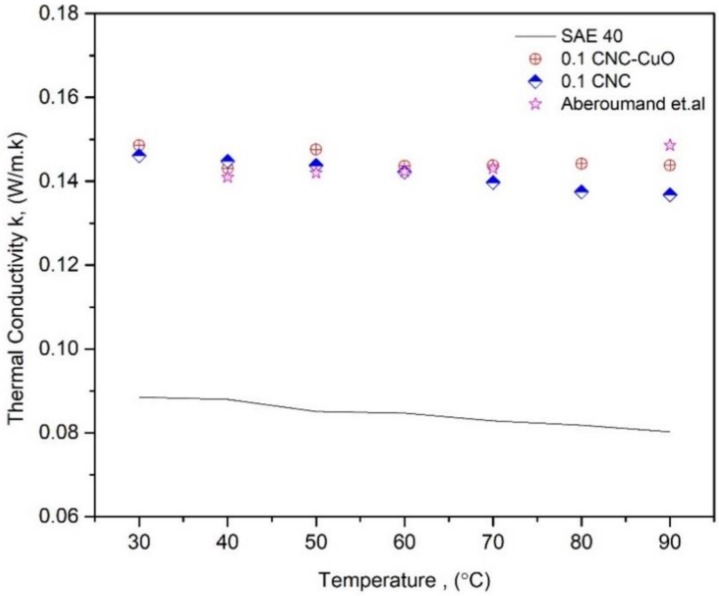

Figure 18 Thermal conductivity result of CNC, CNC-CuO and CuO nanolubricant [73] better than the base fluid

Figure 19 displays the ratio of thermal conductivity given by, $\left(\frac{k_{eff}}{k_b}\right)$ In a function of temperature for all the corresponding solid concentrations. The ratio improves with temperature and with the increase of solid concentration. The maximum value of the thermal conductivity ratio in the chosen nanolubricant is around 1.80566 for a solid concentration of 0.1% at 90℃. The most important cause for the improvement of thermal conductivity is the existence of a layer in the solid-liquid boundary, and particle clumping provides directly to the improvement of thermal conductivity. The molecules of lubricant appear closer to the element and forms encrusted shapes. It behaves like a solid surface and plays a role as a thermal bridge between particles and oil molecules. Furthermore, the thermal conductivity of particles is higher than the lubricant. As the concentration rises, the particles are close enough to improve the phenomenon of heat transfer among the nanoparticles due to a rise in Brownian movements [75].

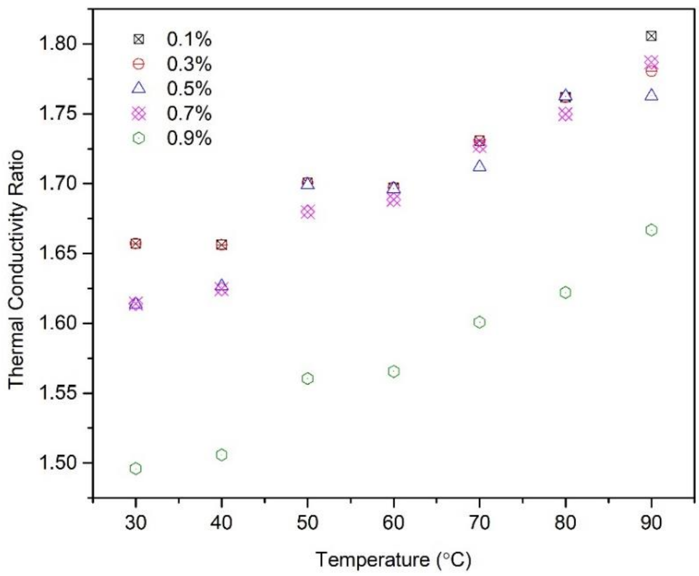

Figure 19 Thermal conductivity ratio of CNC-CuO nanolubricant with the temperature at different concentrations

3.4.2 Comparison concerning Hypothetical Model and Experimental Data

Hypothetical simulations to forecast the thermal conductivity of nanolubricant are suggested by many researchers. In this study, the most generally used models, are Hamilton and Crosser and Yu Choi model, are selected to assess their ability to forecast the thermal conductivity of the studied nanolubricant and assess its results with the experimental data. Hamilton-Crosser (H-C) proposed the basic model to measure thermal conductivity at the solid-liquid condition. The models predict the thermal conductivity at the solid phase ratio greater than 100 [76]. Another method to calculate thermal conductivity was also proposed by Yu and Choi [77]. Table 3 shows the description of the theoretical model.

Table 3 Theoretical model from previous researchers with the description

Model	Description	Proposed by
$$k_{eff} = \left(\frac{k_p + (n-1)k_f + (n-1)\emptyset(k_p - k_f)}{k_p + (n-1)k_f - \emptyset(k_p - k_f)}\right)k_f$$	The model assumption is the discontinuous phase is spherical	[76]
$$k_{eff} = \left(\frac{kp + 2kf + 2\emptyset(kp - kf)(1+\beta)2}{kp + 2kf - \emptyset(kp - kf)(1+\beta)3}\right)kf$$	Modified Maxwell's equation, introducing the effect of the interfacial layer. They assume that the nanolayer impact is significant for small particles (r – h)	[77]

From both equations, the empirical shape factor (n) is as below:

$$n = \frac{3}{\varphi} \quad \text{Eq. 9}$$

where the φ denotes the surface area ratio of a sphere with a volume of the surface area nanoparticles, from the H-C equation, the value of n is 2 (spherical nanoparticles) β in denotes the ratio of the thickness of nanolayer with the real particle radius, these two equations then were used to compare the enhance thermal conductivity ratio. Figure 20 compares the theoretical model with the current experimental data. It is obvious from the figure that both of the equations from the previous study's H-C and Yu-Choi models underestimate the viable thermal conductivity of the nanolubricant. The reason is because of the impact of prime parameters; for example, the nanoparticle size and the interfacial layer were not acknowledged on the thermal conductivity of the nanolubricant. The effective thermal conductivity of nanolubricant relies upon the nanoparticles' thermal conductivity as well as the base fluid, the concentration of nanoparticles, shape and thickness of nanoparticles. Table 4 shows the error analysis of thermal conductivity model and experimental result.

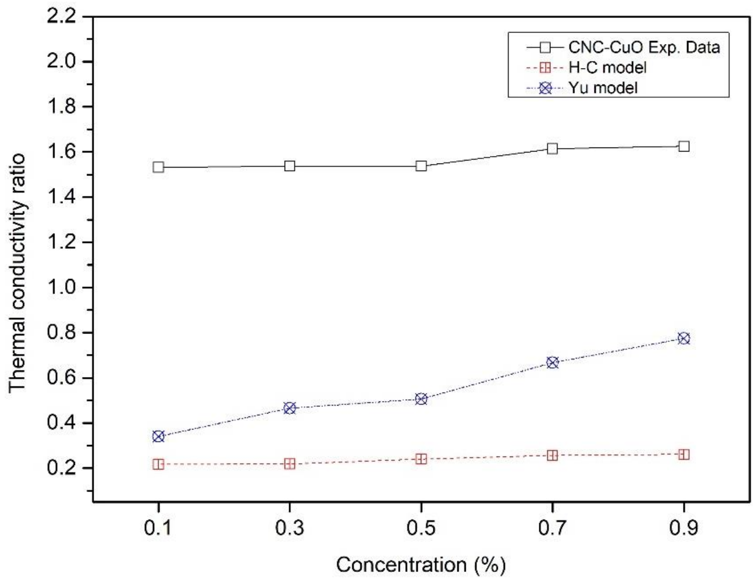

Figure 20 Comparison between theoretical from the previous researcher compared to CNC-CuO experimental data.

Table 4: Error analysis between previous researcher model and experimental thermal conductivity model in percentage

Concentration	H-C Model (%)	Yu Model (%)
0.1	77.99093	70.61376
0.3	78.46741	63.52852
0.5	76.48986	60.84944
0.7	76.93715	54.01294
0.9	76.8401	47.96168

3.5 Specific Heat Capacity

The specific heat (C_p) is the main property of thermophysical for the thermal model. It can be said that specific heat is necessary for assessing a specific-phase heat transfer. The specific heat is also utilized to evaluate additional properties such as thermal expansion coefficient and isothermal compressibility [78]. Thus, specific heat measurements and corresponding models are required to apply the nanolubricants to heat transfer applications. In the present study, similar to thermal conductivity, the specific heat capacity enhancement of CNC-CuO nanolubricants was investigated under three conditions; (i) Different concentrations of nanoparticles dispersed in engine oil. (ii) Nanolubricants at optimum concentration with the variation of temperature, and (iii) Nanolubricants with various types of nanolubricant at constant volume concentration.

3.5.1 Specific Heat Capacity at Different Temperatures and Solid Concentration

Figure 21 displays the difference in experimental findings for median specific heat capacity versus temperature in the base fluid (SAE 40) and CNC-CuO nanolubricant at different concentrations. Oil, in addition to a higher specific heat capacity rate, shows a reduced temperature rise for the total absorption of heat energy; hence, the greater value of *Cp* in the lubricant is improved in heat transfer [79]. Hence, the specific heat capacity of the nanolubricants is an essential criterion for enhancing the load-carrying threshold of the system. The temperatures in the supporting gaps of the bearings are lesser in the place where the specific heat capacity of engine oil is elevated; hence, the heat capacity is elevated in the same operational situation [80]. According to figure 21, 0.1%, 0.3%, and 0.5% show a better value of the *Cp* than the base oil, while 0.7% and 0.9% are below the base fluid. This result indicates that 0.5% is the optimum concentration for better Cp. Figure 22 displays the specific heat capacity against concentration. The specific heat capacity (*Cp*) of fluid significantly affects regulating heat amount or rate of heat transfer in thermal systems. From Figure 23, the specific heat capacity of the nanolubricant decreases as volume concentration improves. This reduction in specific heat with improving volume concentration is constant with the findings in the literature on numerous nanofluids [81, 82].

According to both graphs, after 0.5% concentration, the increase in nanoparticle volume concentration in nanolubricants will certainly decrease the specific heat capacity of the nanolubricants. The specific heat capacity of nanolubricant tends to lessen marginally with a temperature rise. Thus, the rise in the specific heat with temperature examined in Figure 23 is in line with the number of nanoparticles that appeared in the base fluids. The flawed geometric character of the nanoparticles impacts the specific heat of nanoparticles, eventually producing a discrepancy between the specific heat capacity of the particles and the bulk material [83]. As heat increases, the specific heat capacity of the nanoparticles rises and can go beyond that of the bulk material by twice as much [84]. The bigger difference in the straight-line exhibited by the 50/50 lubricant/surfactant blend as associated with the base lubricant is theorized to be affected by some surfactant aggregation. Surfactants have a larger propensity for accumulation at high concentrations [85].

Figure 23 shows the comparison between base oil (SAE 40) with a single nanoparticle: CNC nanolubricant, CNC-CuO nanolubricant and Saeedinia et al [86] conduct the specific heat capacity experiment for CuO nanoparticle with the base oil. According to the graph, the specific heat capacity was improved when nanoparticles were added. This might be due to the nanoparticle size, where CuO shows the smallest size, followed by CNC-CuO and CNC. Greater specific heat capacities for nanoparticles are likely when particles' size is reduced [84, 85]. In a previous study of nanoparticles, specific heat rates are only available up to 80°C, suggesting that the high operating temperatures of nanolubricants have many hidden areas that need to be examined further. A high surface area per unit mass of nanoparticles is recommended to improve the interfacial thermal resistance among the nanoparticles and neighbouring liquid molecules. This elevated interfacial thermal resistance performs as extra thermal space due to the interfacial contact of the vibration energies among nanoparticle atoms and the interfacial molecules. This occurrence can cause a rise in the specific heat of nanolubricant [86].

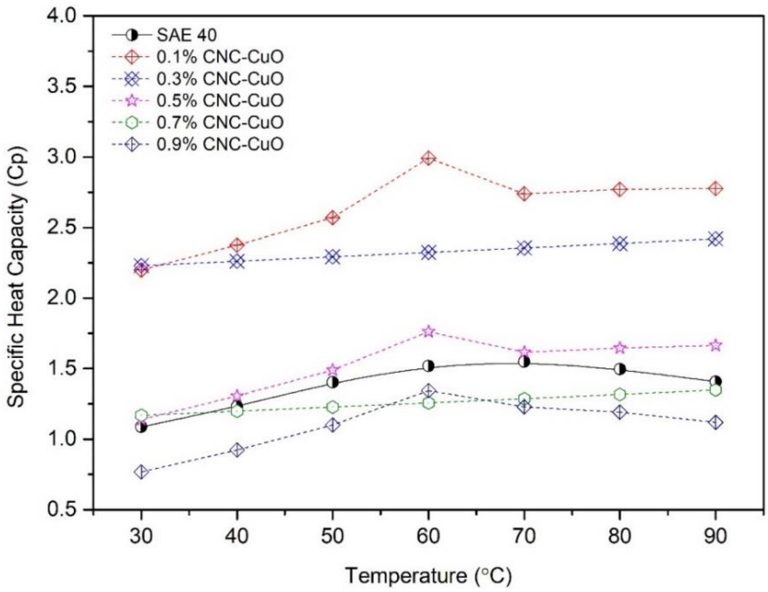

Figure 21 Specific heat capacity of CNC-CuO at different concentrations

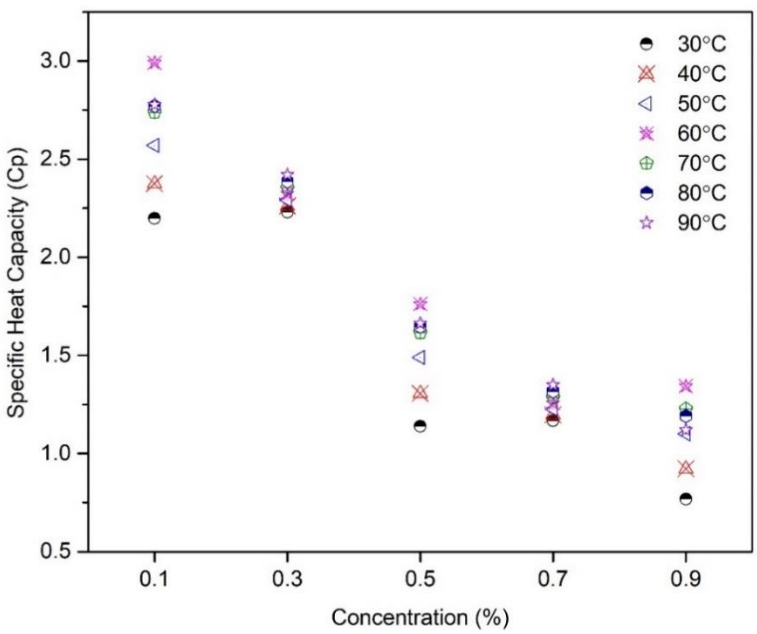

Figure 22 Specific heat capacity at different concentration

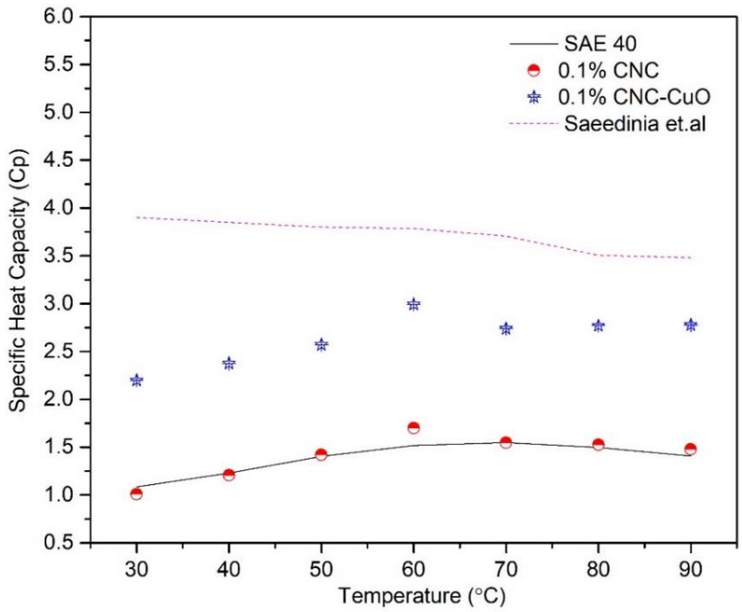

Figure 23 Comparison between specific heat capacity of CNC-CuO with the base fluid (SAE 40), CNC nanolubricant and [87] at 0.1% concentration

3.5.2 Comparison between Theoretical Model and Experimental

As mentioned before, the experiments and models about specific heat capacity are not widely discussed. Forecasting the specific heat capacity of the nanofluids can help investigators enhance their knowledge of the heat holding properties of the nanofluids. Here, two generally used models, Pak and Cho and Xuan and Rotzel, are selected to analyze their ability to forecast the specific heat capacity of the studied nanolubricant and evaluate their results with the experimental data. Table 5 shows the chosen theoretical models. Like thermal conductivity, predicting the specific heat capacity of nanolubricant depends on numerous important parameters, such as nanoparticles concentration, the temperature of nanolubricants and the type of nanoparticle material.

Table 5 Theoretical model for specific heat capacity.

Model	Description	Proposed by
$\boldsymbol{Cpnf, Pak\ and\ Cho = \emptyset Cpp + (1-\emptyset)Cpf}$	The specific heat capacity model significantly deviates from the experimental.	[88]
$\boldsymbol{(\rho Cp)nf, Xuan\ and\ Rotzel = \emptyset(\rho Cp) + (1-\emptyset)(\rho Cp)f}$	Extension of Maxwell's equation, introducing empirical factor n, where n ¼ 3/J and J is particle sphericity.	[89]

According to Table 5, the [88] model is the volume fraction weighted model, and the [89] model is the mass fraction weighted model. The first model assumes that the specific heat is equivalent to the volume fraction weighted average of the specific heats of the base fluid and nanoparticles. This is similar to the mixing theory for ideal gas mixtures. The mass fraction weighted model's second mode is centered on thermal equilibrium. The specific heat corresponds to the mass fraction weighted average of the specific heat of the base fluid and the nanoparticles. The two models generate similar results for tiny nanoparticle concentrations but differ significantly as the nanoparticle concentration rises. Figure 24 shows both models' specific heat capacity ratios compared with experimental data. Figure 24 Xuan and Rotzel model shows the closest to the experimental data compared to Pak and Cho model. This data complies with the previous researchers. Researchers have shown that the mass fraction weighted model exhibits better agreement for nanofluid-specific heat data [90-93]. Table 6 shows the error analysis between model for specific heat capacity with the experimental data.

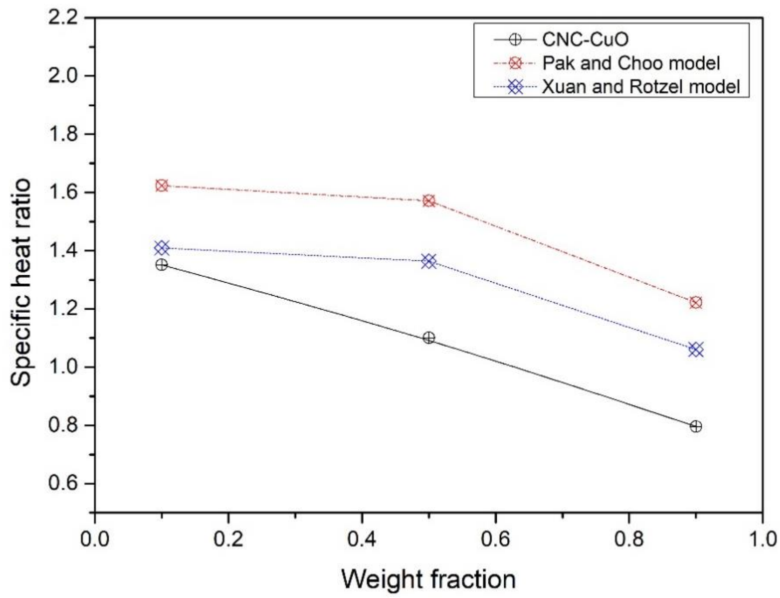

Figure 24 Specific heat ratio at different literature models for CNC-CuO nanolubricant

Table 6: Error analysis between previous researcher model and experimental for specific heat capacity model in percentage (%)

Concentration	Pak and Cho Model	Xuan and Rotzel Model
0.1	20.33761171	4.915597073
0.3	31.32113058	14.20325588
0.5	41.52994184	23.07747541
0.7	46.14309876	27.43899236
0.9	51.79905878	33.20940229

According to [94], for small nanoparticle concentration, the models will exhibit nearly the same result as the experimental but diverge greatly as the concentration increases. The classical numerical calculations do not correctly foresee the experimentally achieved values of specific heat capacity and viscosity. This is because the models do not contain all the aspects impacting the rheological performances in the nanofluids. Based on other research, the thermal equilibrium models, which presume that a thermal equilibrium occurs among the base fluid and the nanoparticles, are a better numerical forecaster of specific heat capacity than the blending concept. Lately, the ‘‘nanolayer effect” has been contemplated in some models for the specific heat of molten-salt nanofluids. The nanolayer effect implies the trend of liquid molecules creating an ordered, thin (a few nanometers), solid-like layer on the nanoparticle shell. This is believed to impact the heat exchange between the liquid and the nanoparticle [95].

Even though there are few findings on the nanolayer effect, it is crucial in verifying nanofluids' thermal conductivity, but its importance for the specific heat is not well realized. Nonetheless, a few findings have indicated that the nanolayer effect in specific heat is particle size-dependent, i.e., the result is further important for tinier nanoparticles [36]. As the measurements have indicated that the particle size does not have an apparent impact on the specific heat it is acceptable to hypothesize that the nanolayer effect for the specific heat, can be ignored.

4.0Conclusion

In the present study, the thermophysical properties and the comparison between the theoretical model and the experimental data of the thermophysical properties have been discussed. Furthermore, the effects of temperature and varied concentrations on Stability, dynamic viscosity, thermal conductivity and specific heat capacity of the CNC-CuO nanoparticle added to engine oil have been studied. The experiments were carried out in temperatures ranging from 30ºC to 90ºC and volume concentrations ranging from 0.1% to 0.9%. Based on the experimental measurements, the following can be concluded:

1) The samples were mixed well with no settlement of nanoparticles at the bottom of the test tube at week 1. After the 4th week, the supernatant layer is at the top of the solution. Therefore, CNC-CuO nano lubricant was observed to be stable for up to one month or more
2) According to the UV-Vis spectrophotometer result, 0.1% shows the closest absorbance ratio to one; thus, 0.1% concentration shows the most stable nano lubricant compared followed by 0.5%, and the least stable nano lubricant is 0.3% concentration.
3) According to the viscosity index result (VI), as the concentration of CNC-CuO nanoparticles increases, the VI is higher, proving that CNC-CuO nanoparticles added with engine oil did improve the lubricity of the base oil regarding its viscosity by 44.3%-47.12%.

4) The minimum and maximum enhancement in the dynamic viscosity was 1.34% and 74.81%, respectively, which occurred at the temperature of 40°C and 90°C and solid concentrations of 0.5% and 0.3%, respectively
5) The thermal conductivity ratio increase with temperature and with the increase of solid concentration as well. The maximum increase of thermal conductivity ratio of the selected nanolubricant was found to be 1.80566 for a solid concentration of 0.1% at 90°C.
6) For specific heat capacity, 0.1%, 0.3% and 0.5% show a better value of the *Cp* than the base oil, while 0.7% and 0.9% are below the base fluid. This result indicates that 0.5% is the optimum concentration for better *Cp*.
7) The main findings of the stability and thermophysical properties of CNC-CuO are usable for the tribology application in terms of determining how to improve engine oil efficiency through the heat transfer and flow behaviour of nanolubricants

4.1 Credit authorship contribution statement

Sakinah Hisham: Conceptualization, Methodology, Validation, Formal analysis, Investigation, Data Curation, Writing - Original Draft, Visualization. **K. Kadirgama, D. Ramasamy:** Conceptualization, Methodology, Validation, Formal analysis, Investigation, Resources, Writing - Review & Editing, Visualization, Supervision. **Mohd Kamal Kamarulzaman, R. Saidur:** Conceptualization, Investigation. **Talal Yusaf:** Review & Editing

4.2 Declaration of competing interest

The authors declare that they have no known competing financial interests or personal relationships that could have appeared to influence the work reported in this paper.

4.3 Acknowledgements

This work was supported by University Malaysia Pahang grant number RDU213308 and Fundamental Research Grant Scheme No. FRGS/1/2018/TK03/UMP/02/26. "Mohd Kamal bin Kamarulzaman" is the recipient of the UMP Post-Doctoral Fellowship in Research.

4.4 References

1. Vyavhare, K., et al., *Tribochemistry of fluorinated ZnO nanoparticles and ZDDP lubricated interface and implications for enhanced anti-wear performance at boundary lubricated contacts.* Wear, 2021. **474**: p. 203717.
2. Wang, L., et al., *Recent progress in metal-organic frameworks-based hydrogels and aerogels and their applications.* Coordination Chemistry Reviews, 2019. **398**: p. 213016.
3. Kanti, P., et al., *Experimental study on density and thermal conductivity properties of Indian coal fly ash water-based nanofluid.* International Journal of Ambient Energy, 2022. **43**(1): p. 2557-2562.
4. Kanti, P., et al., *Experimental determination of thermophysical properties of Indonesian fly-ash nanofluid for heat transfer applications.* Particulate Science and Technology, 2021. **39**(5): p. 597-606.
5. Yukselen, Y. and A. Kaya, *Zeta potential of kaolinite in the presence of alkali, alkaline earth and hydrolyzable metal ions.* Water, Air, and Soil Pollution, 2003. **145**(1): p. 155-168.
6. Mello, V., et al., *Enhancing Cuo nanolubricant performance using dispersing agents.* Tribology International, 2020. **150**: p. 106338.
7. Ramachandran, K., et al., *Thermophysical properties measurement of nano cellulose in ethylene glycol/water.* Applied Thermal Engineering, 2017. **123**: p. 1158-1165.
8. Ramachandran, K., et al., *Investigation on effective thermal conductivity and relative viscosity of cellulose nanocrystal as a nanofluidic thermal transport through a combined experimental – Statistical approach by using Response Surface Methodology.* Applied Thermal Engineering, 2017. **122**(Supplement C): p. 473-483.
9. Klemm, D., et al., *Nanocelluloses: A new family of nature-based materials.* Angewandte Chemie International Edition, 2011. **50**(24): p. 5438-5466.
10. Mohammadkazemi, F., M. Faria, and N. Cordeiro, *In situ biosynthesis of bacterial nanocellulose-CaCO3 hybrid bionanocomposite: One-step process.* Materials Science and Engineering: C, 2016. **65**(Supplement C): p. 393-399.
11. Dong, S., et al., *Nanocellulose crystals derivative-silica hybrid sol open tubular capillary column for enantioseparation.* Carbohydrate Polymers, 2017. **165**(Supplement C): p. 359-367.
12. Azman, N.F. and S. Samion, *Dispersion stability and lubrication mechanism of nanolubricants: a review.* International journal of precision engineering and manufacturing-green technology, 2019. **6**(2): p. 393-414.
13. Mousavi, S.B., S.Z. Heris, and P. Estellé, *Experimental comparison between ZnO and MoS 2 nanoparticles as additives on performance of diesel oil-based nano lubricant.* Scientific reports, 2020. **10**(1): p. 1-17.
14. Pourpasha, H., et al., *The effect of multi-wall carbon nanotubes/turbine meter oil nanofluid concentration on the thermophysical properties of lubricants.* Powder Technology, 2020. **367**: p. 133-142.
15. Kadirgama, K., et al., *Enhancement of tribological behaviour and thermal properties of hybrid nanocellulose/copper (II) oxide nanolubricant.* Journal of Advanced Research in Fluid Mechanics and Thermal Sciences, 2020. **72**(1): p. 47-54.
16. Apmann, K., et al., *Thermal Conductivity and Viscosity: Review and Optimization of Effects of Nanoparticles.* Materials, 2021. **14**(5): p. 1291.
17. Yashawantha, K., et al., *Rheological behavior and thermal conductivity of graphite–ethylene glycol nanofluid.* Journal of Testing and Evaluation, 2019. **49**(4).
18. Awang, N., et al., *An experimental study on characterization and properties of nano lubricant containing Cellulose Nanocrystal (CNC).* International Journal of Heat and Mass Transfer, 2019. **130**: p. 1163-1169.
19. Ren, B., et al., *Tribological properties and anti-wear mechanism of ZnO@ graphene core-shell nanoparticles as lubricant additives.* Tribology International, 2020. **144**: p. 106114.
20. Sulgani, M.T. and A. Karimipour, *Improve the thermal conductivity of 10w40-engine oil at various temperature by addition of Al2O3/Fe2O3 nanoparticles.* Journal of Molecular Liquids, 2019. **283**: p. 660-666.

21. Yang, L., et al., *Enhancing the thermal conductivity of SAE 50 engine oil by adding zinc oxide nano-powder: an experimental study.* Powder Technology, 2019. **356**: p. 335-341.
22. Arani, A.A.A., et al., *Statistical analysis of enriched water heat transfer with various sizes of MgO nanoparticles using artificial neural networks modeling.* Physica A: Statistical Mechanics and its Applications, 2020. **554**: p. 123950.
23. Esfe, M.H., et al., *Experimental investigation and model development of the non-Newtonian behavior of CuO-MWCNT-10w40 hybrid nano-lubricant for lubrication purposes.* Journal of Molecular Liquids, 2018. **249**: p. 677-687.
24. Esfe, M.H., A.T.K. Abad, and M. Fouladi, *Effect of suspending optimized ratio of nano-additives MWCNT-Al2O3 on viscosity behavior of 5W50.* Journal of Molecular Liquids, 2019. **285**: p. 572-585.
25. Alarifi, I.M., et al., *Feasibility of ANFIS-PSO and ANFIS-GA models in predicting thermophysical properties of Al2O3-MWCNT/oil hybrid nanofluid.* Materials, 2019. **12**(21): p. 3628.
26. Mubina, M.K., et al., *Enriched biological and mechanical properties of boron doped SiO2-CaO-Na2O-P2O5 bioactive glass ceramics (BGC).* Journal of Non-Crystalline Solids, 2021. **570**: p. 121007.
27. Zainon, S. and W. Azmi, *Recent Progress on Stability and Thermo-Physical Properties of Mono and Hybrid towards Green Nanofluids.* Micromachines, 2021. **12**(2): p. 176.
28. Jatti, V.S. and T. Singh, *Copper oxide nano-particles as friction-reduction and anti-wear additives in lubricating oil.* Journal of Mechanical Science and Technology, 2015. **29**(2): p. 793-798.
29. Borda, F.L.G., et al., *Experimental investigation of the tribological behavior of lubricants with additive containing copper nanoparticles.* Tribology International, 2018. **117**: p. 52-58.
30. Choi, Y., et al., *Tribological behavior of copper nanoparticles as additives in oil.* Current Applied Physics, 2009. **9**(2): p. e124-e127.
31. Kole, M. and T. Dey, *Enhanced thermophysical properties of copper nanoparticles dispersed in gear oil.* Applied thermal engineering, 2013. **56**(1-2): p. 45-53.
32. Gupta, M., et al., *Up to date review on the synthesis and thermophysical properties of hybrid nanofluids.* Journal of cleaner production, 2018. **190**: p. 169-192.
33. Esfe, M.H., et al., *Application of three-level general factorial design approach for thermal conductivity of MgO/water nanofluids.* Applied Thermal Engineering, 2017. **127**: p. 1194-1199.
34. Suganthi, K., et al., *Cerium oxide–ethylene glycol nanofluids with improved transport properties: preparation and elucidation of mechanism.* Journal of the Taiwan Institute of Chemical Engineers, 2015. **49**: p. 183-191.
35. Mariano, A., et al., *Co3O4 ethylene glycol-based nanofluids: thermal conductivity, viscosity and high pressure density.* International Journal of Heat and Mass Transfer, 2015. **85**: p. 54-60.
36. Yu, W., et al., *Comparative review of turbulent heat transfer of nanofluids.* International journal of heat and mass transfer, 2012. **55**(21-22): p. 5380-5396.
37. Yuan, Y., et al., *Spray drying assisted assembly of ZnO nanocrystals using cellulose as sacrificial template and studies on their photoluminescent and photocatalytic properties.* Colloids and Surfaces A: Physicochemical and Engineering Aspects, 2017. **522**: p. 173-182.
38. Awang, N.W., et al., *An experimental study on characterization and properties of nano lubricant containing Cellulose Nanocrystal (CNC).* International Journal of Heat and Mass Transfer, 2019. **130**: p. 1163-1169.
39. Xia, W., et al., *Analysis of oil-in-water based nanolubricants with varying mass fractions of oil and TiO2 nanoparticles.* Wear, 2017.
40. Sezer, N., M.A. Atieh, and M. Koç, *A comprehensive review on synthesis, stability, thermophysical properties, and characterization of nanofluids.* Powder Technology, 2019. **344**: p. 404-431.
41. Li, X., et al., *Experimental investigation of β-cyclodextrin modified carbon nanotubes nanofluids for solar energy systems: Stability, optical properties and thermal conductivity.* Solar Energy Materials and Solar Cells, 2016. **157**: p. 572-579.

42. Almanassra, I.W., et al., *An experimental study on stability and thermal conductivity of water/CNTs nanofluids using different surfactants: A comparison study.* Journal of Molecular Liquids, 2019: p. 111025.
43. Mukesh Kumar, P.C., K. Palanisamy, and V. Vijayan, *Stability analysis of heat transfer hybrid/water nanofluids.* Materials Today: Proceedings, 2019.
44. Suryawanshi, A., et al. *Experimental Investigation of Tribological Properties of Engine oil with CuO Nanoparticles Under Varying Loading Conditions*. in *An International Conference on Tribology, TRIBOINDIA-2018, 13th-15th*. 2018.
45. Abd-Elghany, M. and T.M. Klapötke, *A review on differential scanning calorimetry technique and its importance in the field of energetic materials.* Physical Sciences Reviews, 2018. **3**(4).
46. Peng, B., et al., *A review of nanomaterials for nanofluid enhanced oil recovery.* RSC advances, 2017. **7**(51): p. 32246-32254.
47. Sui, T., et al., *Effect of particle size and ligand on the tribological properties of amino functionalized hairy silica nanoparticles as an additive to polyalphaolefin.* Journal of Nanomaterials, 2015. **2015**.
48. Dubey, M.K., J. Bijwe, and S. Ramakumar, *PTFE based nano-lubricants.* Wear, 2013. **306**(1-2): p. 80-88.
49. Hardesty, J.H. and B. Attili, *Spectrophotometry and the Beer-Lambert Law: An important analytical technique in chemistry.* Collin College, Department of Chemistry, 2010.
50. Richardson, J.F. and W.N. Zaki, *The sedimentation of a suspension of uniform spheres under conditions of viscous flow.* Chemical Engineering Science, 1954. **3**(2): p. 65-73.
51. Kotia, A., et al., *Effect of copper oxide nanoparticles on thermophysical properties of hydraulic oil-based nanolubricants.* Journal of the Brazilian Society of Mechanical Sciences and Engineering, 2017. **39**(1): p. 259-266.
52. Sharma, G., et al., *Kinematic Viscosity Prediction of Nanolubricants Employed in Heavy Earth Moving Machinery Using Machine Learning Techniques.* International Journal of Precision Engineering and Manufacturing, 2020. **21**(10): p. 1921-1932.
53. Talib, N., R. Nasir, and E. Rahim, *Tribological behaviour of modified jatropha oil by mixing hexagonal boron nitride nanoparticles as a bio-based lubricant for machining processes.* Journal of Cleaner Production, 2017. **147**: p. 360-378.
54. Ali, M.K.A., et al., *Improving the tribological characteristics of piston ring assembly in automotive engines using Al2O3 and TiO2 nanomaterials as nano-lubricant additives.* Tribology International, 2016. **103**: p. 540-554.
55. Stachowiak, G. and A.W. Batchelor, *Experimental methods in tribology*. Vol. 44. 2004: Elsevier.
56. Srivatsa, J.T. and M.B. Ziaja, *An Experimental Investigation on Use of Nanoparticles as Fluid Loss Additives in a Surfactant - Polymer Based Drilling Fluids*. International Petroleum Technology Conference.
57. Klamann, D., R. Rost, and A. Killer, *Lubricants and related products: synthesis, properties, applications, international standards*. 1984: Verlag Chemie Weinheim.
58. Chaurasia, S.K., N.K. Singh, and L.K. Singh, *Friction and wear behavior of chemically modified Sal (Shorea Robusta) oil for bio based lubricant application with effect of CuO nanoparticles.* Fuel, 2020. **282**: p. 118762.
59. Zhao, Z. and C. Wang, *Cryogenic Engineering and Technologies: Principles and Applications of Cryogen-Free Systems*. 2019: CRC Press.
60. Kabelac, S. and J. Kuhnke. *Heat transfer mechanisms in nanofluids--experiments and theory*. in *International Heat Transfer Conference 13*. 2006. Begel House Inc.
61. Prasher, R., et al., *Measurements of nanofluid viscosity and its implications for thermal applications.* Applied physics letters, 2006. **89**(13): p. 133108.
62. Esfe, M.H., A.A.A. Arani, and S. Esfandeh, *Improving engine oil lubrication in light-duty vehicles by using of dispersing MWCNT and ZnO nanoparticles in 5W50 as viscosity index improvers (VII).* Applied Thermal Engineering, 2018. **143**: p. 493-506.
63. Goodarzi, M., et al., *Experimental evaluation of dynamic viscosity of ZnO–MWCNTs/engine oil hybrid nanolubricant based on changes in temperature and concentration.* Journal of Thermal Analysis and Calorimetry, 2019. **136**(2): p. 513-525.

64. Esfe, M.H., et al., *Examination of rheological behavior of MWCNTs/ZnO-SAE40 hybrid nano-lubricants under various temperatures and solid volume fractions.* Experimental Thermal and Fluid Science, 2017. **80**: p. 384-390.
65. Einstein, A., *Eine neue Bestimmung der Moleküldimensionen.* Annalen der Physik, 1906. **324**(2): p. 289-306.
66. Batchelor, G., *The effect of Brownian motion on the bulk stress in a suspension of spherical particles.* Journal of fluid mechanics, 1977. **83**(1): p. 97-117.
67. Wang, X., X. Xu, and S.U. Choi, *Thermal conductivity of nanoparticle-fluid mixture.* Journal of thermophysics and heat transfer, 1999. **13**(4): p. 474-480.
68. Maïga, S.E.B., et al., *Heat transfer enhancement by using nanofluids in forced convection flows.* International Journal of Heat and Fluid Flow, 2005. **26**(4): p. 530-546.
69. Afrand, M., K.N. Najafabadi, and M. Akbari, *Effects of temperature and solid volume fraction on viscosity of SiO2-MWCNTs/SAE40 hybrid nanofluid as a coolant and lubricant in heat engines.* Applied Thermal Engineering, 2016. **102**: p. 45-54.
70. Hemmat Esfe, M., A.A. Abbasian Arani, and S. Esfandeh, *Improving engine oil lubrication in light-duty vehicles by using of dispersing MWCNT and ZnO nanoparticles in 5W50 as viscosity index improvers (VII).* Applied Thermal Engineering, 2018. **143**: p. 493-506.
71. Ahmadi, H., et al., *Preparation and thermal properties of oil-based nanofluid from multi-walled carbon nanotubes and engine oil as nano-lubricant.* International Communications in Heat and Mass Transfer, 2013. **46**: p. 142-147.
72. Farbod, M., R. Kouhpeymani asl, and A.R. Noghreh abadi, *Morphology dependence of thermal and rheological properties of oil-based nanofluids of CuO nanostructures.* Colloids and Surfaces A: Physicochemical and Engineering Aspects, 2015. **474**: p. 71-75.
73. Aberoumand, S. and A. Jafarimoghaddam, *Experimental study on synthesis, stability, thermal conductivity and viscosity of Cu–engine oil nanofluid.* Journal of the Taiwan Institute of Chemical Engineers, 2017. **71**: p. 315-322.
74. Domingues, G., et al., *Heat transfer between two nanoparticles through near field interaction.* Physical review letters, 2005. **94**(8): p. 085901.
75. Narayanasarma, S. and B.T. Kuzhiveli, *Evaluation of the properties of POE/SiO2 nanolubricant for an energy-efficient refrigeration system–An experimental assessment.* Powder Technology, 2019. **356**: p. 1029-1044.
76. Hamilton, R.L. and O. Crosser, *Thermal conductivity of heterogeneous two-component systems.* Industrial & Engineering chemistry fundamentals, 1962. **1**(3): p. 187-191.
77. Yu, W. and S. Choi, *The role of interfacial layers in the enhanced thermal conductivity of nanofluids: a renovated Maxwell model.* Journal of nanoparticle research, 2003. **5**(1-2): p. 167-171.
78. Gaskell, D.R. and D.E. Laughlin, *Introduction to the Thermodynamics of Materials*. 2017: CRC press.
79. Salgado, J., et al., *Isobaric heat capacity of nanostructured liquids with potential use as lubricants.* The Journal of Chemical Thermodynamics, 2018. **123**: p. 107-116.
80. Duangthongsuk, W. and S. Wongwises, *Comparison of the effects of measured and computed thermophysical properties of nanofluids on heat transfer performance.* Experimental Thermal and Fluid Science, 2010. **34**(5): p. 616-624.
81. Wole-Osho, I., et al., *An experimental investigation into the effect of particle mixture ratio on specific heat capacity and dynamic viscosity of Al2O3-ZnO hybrid nanofluids.* Powder Technology, 2020. **363**: p. 699-716.
82. Lee, J. and I. Mudawar, *Assessment of the effectiveness of nanofluids for single-phase and two-phase heat transfer in micro-channels.* International Journal of Heat and Mass Transfer, 2007. **50**(3-4): p. 452-463.
83. Likhachev, V., G. Vinogradov, and M. Alymov, *Anomalous heat capacity of nanoparticles.* Physics Letters A, 2006. **357**(3): p. 236-239.
84. Wang, B.-X., L.-P. Zhou, and X.-F. Peng, *Surface and size effects on the specific heat capacity of nanoparticles.* International journal of thermophysics, 2006. **27**(1): p. 139-151.

85. Aparna, Z., et al., *Thermal conductivity of aqueous Al2O3/Ag hybrid nanofluid at different temperatures and volume concentrations: an experimental investigation and development of new correlation function.* Powder Technology, 2019. **343**: p. 714-722.
86. Shin, D. and D. Banerjee. *Experimental investigation of molten salt nanofluid for solar thermal energy application.* in *ASME/JSME Thermal Engineering Joint Conference*. 2011.
87. Saeedinia, M., M. Akhavan-Behabadi, and P. Razi, *Thermal and rheological characteristics of CuO–Base oil nanofluid flow inside a circular tube.* International Communications in Heat and Mass Transfer, 2012. **39**(1): p. 152-159.
88. Pak, B.C. and Y.I. Cho, *Hydrodynamic and heat transfer study of dispersed fluids with submicron metallic oxide particles.* Experimental Heat Transfer an International Journal, 1998. **11**(2): p. 151-170.
89. Xuan, Y. and Q. Li, *Investigation on convective heat transfer and flow features of nanofluids.* Journal of Heat transfer, 2003. **125**(1): p. 151-155.
90. Álvarez-Miranda, E. and J. Pereira, *On the complexity of assembly line balancing problems.* Computers & Operations Research, 2019. **108**: p. 182-186.
91. Assessment, U.O.o.T. and U.S.C.O.o.T. Assessment. *Biopolymers: Making Materials Nature's Way*. 1993. Congress.
92. Chandra, R. and R. Rustgi, *Department of Polymer Technology and Applied Chemistry,".* Biodegradable Polymers", Delhi College of Engineering, India, 1998: p. 1273-1335.
93. Chinet, F.S. and M. Godinho Filho, *POLCA System: literature review, classification, and analysis.* Gestão & Produção, 2014. **21**(3): p. 532-542.
94. Lin, L. and M.A. Kedzierski, *Specific heat of aluminum-oxide nanolubricants.* International Journal of Heat and Mass Transfer, 2018. **126**: p. 1168-1176.
95. Qu, F., C. Yan, and D. Sun, *Investigation into the influences of the low speed's accuracy on the hypersonic heating computations.* International Communications in Heat and Mass Transfer, 2016. **70**: p. 53-58.